Università degli studi di Pisa
Facoltà di Scienze Matematiche, Fisiche e Naturali

Corso di Laurea in Fisica

Tesi di Laurea Magistrale

Super-Adiabatic Transfer in Three-level Systems

Relatore
Prof. Ennio Arimondo

Candidato
Luigi Giannelli

Anno accademico 2012/2013

Contents

Introduction

The search for techniques with which to control the transfer of population between specified quantum states is a major theme of atomic and molecular physics and is a fundamental requirement in many areas of modern science [1] such as quantum information processing [2], metrology, interferometry, or driving of chemical reactions. In particular in this work the three-level system is analysed in the ladder ($E_1 < E_2 < E_3$) or Λ ($E_1 < E_2$, $E_3 < E_2$) configuration (see fig. 2.1). The generic goal is to study and optimise the population transfer from the initial state $|1\rangle$ to the finale state $|3\rangle$ of the same parity, for which single-photon transitions are forbidden for electric dipole radiation.

The use of two consecutive laser pulses, each of them inverting the population (π-pulses), serve the purpose, but the result is highly sensitive to the deviations of pulse areas, exact laser resonances, and decay and perturbations of the intermediate level $|2\rangle$, through which the whole population has to pass. A popular method for the transfer of population in a three-level system is the technique of stimulated emission pumping (SEP) (see [3]). With SEP the pump laser, that links the initial populated state $|1\rangle$ with an intermediate state $|2\rangle$, acts first, followed, after some time delay, by the Stokes laser that links the intermediate state $|2\rangle$ with the final, target, state $|3\rangle$. If the lasers intensities are sufficiently high to saturate the respective transitions, at the end of the process 50% of the population is found in level $|1\rangle$, 25% in level $|2\rangle$ and 25% in level $|3\rangle$. SEP is relatively easy to implement but it suffers of some problems: lasers' intensities must be high enough to saturate respective transitions, only 25% of the population may be found in the final state $|3\rangle$ and the possibility of radiative decay from the intermediate state $|2\rangle$ to states other than the desired final state may be detrimental to the implementation of an efficient transfer.

It has long been recognised, however, that adiabatic procedures, in which an atom remains at all times in one eigenstate of a smoothly changing Hamiltonian, offer opportunities for a complete population transfer without the need of an accurate control of the experimental parameters (such as the pulse shapes). An interesting and far reaching alternative to SEP, one which exploits the coherence of the radiation fields, is the so called *'stimulated Raman adiabatic passage'* (STIRAP, for a review see [4, 5]). With STIRAP, based on the adiabatic evolution of a dark state, the system first interacts with the so-called Stokes laser connecting the final states, and then with the so-called pump

laser connecting the initial and intermediate states (there must be an appropriate overlap between them). This is often termed counter-intuitive pulse sequence. If the laser intensities are sufficiently high (i.e. if the adiabatic condition is fulfilled), the system follows adiabatically an eigenstate of the Hamiltonian reaching nearly complete transfer of population from state $|1\rangle$ to state $|3\rangle$. The process can be made relatively insensitive to many of the experimental details of the pulses. In addition STIRAP has the remarkable property of placing almost no population into the intermediate state $|2\rangle$, and thus it is also insensitive to any possible decay from that state.

The drawback of this method is the fulfilling of the adiabatic condition that may require high intensities or may slow down the time of the process. There are many instances where speeding up the evolution process may be of practical interest e.g., for applications with many repetitions such as the manipulation of quantum information, or for applications that may suffer from decoherence or noise.

Experimental realizations of the STIRAP process have been done by Cubel et al. [6] exciting ^{85}Rb atoms to $44D_{5/2}$ Rydberg state with a fidelity of 0.5, and by Gearba et al. [7] exciting ^{87}Rb atoms to $4D$ state and reaching a fidelity of 0.9.

This work analyse the possibility to achieve a perfect adiabatic following of an eigenstate of the STIRAP Hamiltonian by the construction of an auxiliary Hamiltonian that exactly cancels the non-adiabatic part of the process, i.e., there is no need of fulfilling the adiabatic condition. This is done in accordance with the theory developed within the last few years by several authors, named transitionless, superadiabatic or shortcut to adiabaticity protocols [8–12]. The experimental verification of a superadiabatic protocol for a two-level system was recently developed by the Pisa laboratory [13–15].

This thesis is mainly theoretical. However the STIRAP protocols developed within my work were tested in the laboratory on ultracold rubidium atoms excited to Rydberg states. I participated to the data collection and analysis for a preliminary experimental investigation.

Experimental tests of the STIRAP process have been done in the BEC lab. The target of the experimental work is to perform for the first time an absolute test of the STIRAP efficiency, accessible to the lab owing to the accurate determination of the number of atoms and the number of Rydberg [16].

The content of this thesis can be outlined as follows:

- Chapter 1: introduction to the theory of adiabatic following of eigenstates and the theory of Super-Adiabatic transitions,
- Chapter 2: an overview of the STIRAP process,
- Chapter 3: the Super-Adiabatic theory applied to STIRAP
- Chapter 4: comparison between various STIRAP pulses and results of numerical simulations,

- Chapter 5: study of the robustness of the STIRAP and of the Super-Adiabatic STIRAP,
- Chapter 6: experimental study and preliminary results.

CHAPTER 1

Adiabatic Versus Super-Adiabatic Evolution

1.1 Adiabatic Theorem

Consider a time-dependent Hamiltonian $H_0(t)$ and its instantaneous eigenstates and eigenvalues

$$\begin{aligned} H_0(t)\,|n(t)\rangle &= E_n(t)\,|n(t)\rangle \\ \langle m(t)|n(t)\rangle &= \delta_{mn} \end{aligned} \tag{1.1}$$

and for simplicity let's assume all the states to be non-degenerate for any t. The solution of the Schrödinger equation

$$\imath\hbar\frac{\partial}{\partial t}\,|\psi(t)\rangle = H_0(t)\,|\psi(t)\rangle \tag{1.2}$$

is in general a linear combination of all instantaneous eigenstates $|n(t)\rangle$

$$|\psi(t)\rangle = \sum_n c_n(t)\,|n(t)\rangle\,. \tag{1.3}$$

If the Hamiltonian is slowly varying and the system starts in one of the $|n(t)\rangle$, then the adiabatic theorem [17] guarantees that the system will follow that instantaneous eigenstate closely: the transition amplitude to instantaneous eigenstates different from the starting one is very small during the evolution. Suppose the starting state is $|\psi(t_i)\rangle = |m(t_i)\rangle$, then

$$|\psi(t)\rangle \simeq e^{i\alpha_m(t)}\,|m(t)\rangle \quad \forall\, t \tag{1.4}$$

It is natural to call the instantaneous eigenstates of the Hamiltonian *adiabatic states.*

1.1.1 Proof of the Adiabatic Theorem

Substituting Eq. (1.3) in Eq. (1.2) we get

$$\begin{aligned} \mathrm{i}\hbar\frac{\partial}{\partial t}\left(\sum_n c_n(t)\,|n(t)\rangle\right) = H_0(t)\sum_n c_n(t)\,|n(t)\rangle \quad \Rightarrow \\ \mathrm{i}\hbar\sum_n\left[\left(\frac{\partial c_n(t)}{\partial t}\right)|n(t)\rangle + c_n(t)\frac{\partial\,|n(t)\rangle}{\partial t}\right] = H_0(t)\sum_n c_n(t)\,|n(t)\rangle\,. \end{aligned} \tag{1.5}$$

Multiplying by $\langle m(t)|$ on the left we have

$$\frac{\partial c_m(t)}{\partial t} = -\frac{\mathrm{i}}{\hbar}E_m(t)c_m(t) - \sum_n c_n(t)\,\langle m(t)|\partial_t n(t)\rangle\,. \tag{1.6}$$

Differentiating Eq. (1.1) and multiplying it by $\langle m(t)|$ (with $m \neq n$) we obtain

$$\begin{aligned} \langle m(t)|\,\frac{\partial H_0(t)}{\partial t}\,|n(t)\rangle + E_m(t)\,\langle m(t)|\partial_t n(t)\rangle = E_n(t)\,\langle m(t)|\partial_t n(t)\rangle \\ \Rightarrow \quad \langle m(t)|\partial_t n(t)\rangle = \frac{\langle m(t)|\,\partial_t H_0(t)\,|n(t)\rangle}{E_n(t) - E_m(t)} \quad \text{for } m \neq n. \end{aligned} \tag{1.7}$$

Eq. (1.6) then became

$$\frac{\partial c_m(t)}{\partial t} = -\left(\frac{\mathrm{i}}{\hbar}E_m(t) + \langle m(t)|\partial_t m(t)\rangle\right)c_m(t) - \sum_{n\neq m}\frac{\langle m(t)|\,\partial_t H_0(t)\,|n(t)\rangle}{E_n(t) - E_m(t)}c_n(t). \tag{1.8}$$

The last term in the above equation contains the time derivative of the Hamiltonian so the adiabatic approximation consists in neglecting this term. Within this approximation the equation for $c_m(t)$ became

$$\frac{\partial c_m(t)}{\partial t} \simeq -\left(\frac{\mathrm{i}}{\hbar}E_m(t) + \langle m(t)|\partial_t m(t)\rangle\right)c_m(t) \tag{1.9}$$

and the solution can be easily found

$$c_m(t) \simeq c_m(t_i)e^{\mathrm{i}\theta_m(t)}e^{\mathrm{i}\gamma_m(t)} \tag{1.10}$$

having defined the dynamic phase factor and the geometric phase respectively as

$$\theta_m(t) = -\frac{1}{\hbar}\int_{t_i}^{t} E_m(t')\,dt' \tag{1.11a}$$

$$\gamma_m(t) = \mathrm{i}\int_{t_i}^{t}\left\langle m(t')\middle|\partial_t m(t')\right\rangle\,dt'. \tag{1.11b}$$

The general solution then is

$$|\psi(t)\rangle \simeq \sum_n c_n(t_i)e^{\mathrm{i}\theta_n(t)}e^{\mathrm{i}\gamma_n(t)}\,|n(t)\rangle\,. \tag{1.12}$$

Suppose the system starts in one instantaneous eigenstate of $H_0(t)$, say $|m(t)\rangle$, i.e.,

$$c_n(t_i) = \delta_{mn} \quad \forall n. \tag{1.13}$$

By solution (1.10) the coefficients $c_n(t)$ in the expansion acquire only a phase factor. This means that $|c_n(t)| = |c_n(0)|$ for all the time of the evolution, i.e., the system remains in that instantaneous eigenstate. In fact, in the adiabatic approximation, the state driven by $H_0(t)$ would be (by substituting Eq. (1.13) in Eq. (1.12))

$$|\psi_m(t)\rangle = e^{\mathrm{i}\theta_m(t)} e^{\mathrm{i}\gamma_m(t)} |m(t)\rangle \tag{1.14}$$

as reported in Eq. (1.4).

1.1.2 Validity of the Adiabatic Approximation

A measure of the error involved in this approximation is given by the probability of finding the system at time t in a state different to $|\psi_m(t)\rangle$

$$p_{m\to n}(t) = |\langle n(t)|\psi(t)\rangle|^2 \quad \text{for } n \neq m \tag{1.15}$$

where $\psi(t)$ is the exact solution of the Schrödinger equation. These probabilities calculated by a perturbation method [18] are

$$p_{m\to n}(t) \simeq \hbar^2 \left| \frac{\langle n(t)|\partial_t m(t)\rangle}{E_n(t) - E_m(t)} \right|^2 . \tag{1.16}$$

The adiabatic theorem may be considered valid if the condition

$$\hbar^2 \left| \frac{\langle n(t)|\partial_t m(t)\rangle}{E_n(t) - E_m(t)} \right|^2 \ll 1 \tag{1.17a}$$

or equivalently

$$|\langle n(t)|\partial_t m(t)\rangle| \ll \frac{|E_n(t) - E_m(t)|}{\hbar} \tag{1.17b}$$

is fulfilled.

1.2 Transitionless Quantum Driving

In a recent article [9] Sir Michael Victor Berry wrote:

> For a general quantum system driven by a slowly time-dependent Hamiltonian, transitions between instantaneous eigenstates are exponentially weak. But a nearby Hamiltonian exists for which the transition amplitudes between any eigenstates of the original Hamiltonian are exactly zero for all values of slowness.

Consider a time-dependent Hamiltonian $H_0(t)$ and its instantaneous eigenstates and eigenvalues as defined in Eq. (1.1) and, once again, for simplicity let's assume all the states to be non-degenerate for any t.

As shown above, the adiabatic theorem states that if the condition of Eq. (1.17) is fulfilled and the system starts in one instantaneous eigenstate of the Hamiltonian, the transition amplitude to other different instantaneous eigenstates is very small, and the system will follow adiabatically the starting eigenstate. Although the transition amplitude is very small, it is not zero.

In the quoted article [9] Berry showed that there exists an Hamiltonian

$$H(t) = H_0(t) + H_1(t) \tag{1.18}$$

that drive the instantaneous eigenstates of $H_0(t)$ exactly: there are no transition between those eigenstates for all values of slowness. The super-adiabatic correction $H_1(t)$ is defined as in the following:

$$H_1(t) = \frac{\mathrm{i}\hbar}{2} \sum_n \left(|\partial_t n(t)\rangle \langle n(t)| - |n(t)\rangle \langle \partial_t n(t)| \right). \tag{1.19}$$

The solution of the Schrödinger equation

$$\mathrm{i}\hbar \frac{\partial}{\partial t} |\psi(t)\rangle = H(t) |\psi(t)\rangle = (H_0(t) + H_1(t)) |\psi(t)\rangle \tag{1.20}$$

with

$$|\psi(t_i)\rangle = |m(t_i)\rangle \tag{1.21}$$

is exactly

$$|\psi(t)\rangle = e^{\mathrm{i}\varphi(t)} |m(t)\rangle \quad \forall\, t \tag{1.22}$$

where $|m(t)\rangle$ is an instantaneous eigenstate of $H_0(t)$ and $\varphi(t) = \theta_m(t) + \gamma_m(t)$. We will call this evolution "super-adiabatic" evolution.

1.3 Super-Adiabatic Transfer in Two-level Systems

In a recent article Bason et al. [13] have investigated the super-adiabatic transfer for two-level systems. Two states $|0\rangle$ and $|1\rangle$, the diabatic levels, are coupled via a time-dependent Landau–Zener Hamiltonian of the form

$$H_{LZ}(\tau) = \Gamma(\tau)\sigma_z + \omega(\tau)\sigma_x. \tag{1.23}$$

where $\sigma_{x,z}$ are the Pauli operators with $\sigma_x |0\rangle = |1\rangle$, and $\tau = t/T$ is the rescaled time, T being the duration of the evolution.

Applying the super-adiabatic definition (1.19) to this system one find that the super-adiabatic correction is

$$H_s(t) = \frac{\hbar}{2} \frac{\partial \phi}{\partial t} \sigma_y \tag{1.24}$$

where

$$\tan\phi(t) = \frac{\omega(t)}{\Gamma(t)} \tag{1.25}$$

This means that to make the evolution of the system perfectly adiabatic one needs to add an interaction term corresponding to a σ_y Pauli matrix. In practice, H_s can be implemented by introducing an additional interaction into the system, for example, through an extra laser or microwave field. It can be shown, however, that for the optical lattice investigation of Ref. [13] the effect of this extra field can also be achieved through an appropriate transformation $\Gamma \to \Gamma'$ and $\omega \to \omega'$, such that no extra field is necessary.

Imposing the condition $\Gamma = \Gamma'$, the *tangent protocol* and its super-adiabatic counterpart is derived

$$\Gamma'(\tau) = \Gamma(\tau) = \omega \tan\left(2\left(\tau - \frac{1}{2}\right)\arctan\left(\frac{2}{\omega}\right)\right) \tag{1.26a}$$

(apart from the delta-functions at the beginning and at the end of the protocol) and

$$\omega' = \omega\sqrt{1 + \frac{\arctan\left(\frac{2}{\omega}\right)^2}{(T\omega)^2}}, \tag{1.26b}$$

here Γ and ω refer to the tangent protocol, while Γ' and ω' refer to the super-adiabatic tangent protocol.

The super-adiabatic tangent protocol is extremely robust to variation in its parameters. In Fig. 1.1 the fidelity is plotted as a function of the relative deviation of T and ω from

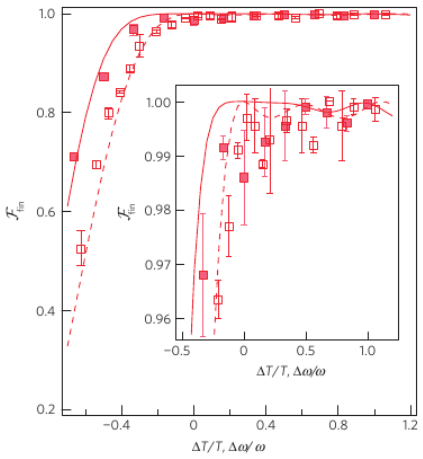

Figure 1.1: Fidelity of the super-adiabatic tangent protocol as a function of the relative deviation of T (filled red squares) and ω (open red squares) from their ideal values. The solid and dashed lines are the respective numerical simulations. Reproduced from Ref. [13].

their ideal values: it is clear that the super-adiabatic tangent protocol is extremely robust with respect to an increase of T and ω.

It is also interesting to study a protocol that minimize the time of the transfer T. Imposing only the constraint that ω be constant (otherwise $T_{min} \to 0$ as $\omega \to \infty$), the protocol that minimize T is the so called *composite pulse protocol*, which can be written

$$\Gamma(\tau) = \begin{cases} -\Gamma_0 & \text{for } \tau = 0 \\ +\Gamma_M & \text{for } \tau \in [0, \tau_0] \\ 0 & \text{for } \tau \in [\tau_0, 1-\tau_0] \\ -\Gamma_M & \text{for } \tau \in [1-\tau_0, 1] \\ +\Gamma_0 & \text{for } \tau = 1 \end{cases} \tag{1.27}$$

where Γ_M and τ_0 being, respectively, asymptotically large and small quantities which satisfy the condition

$$\Gamma_M \tau_0 = \frac{\pi}{4}. \tag{1.28}$$

This composite pulse protocol represents a π-pulse, i.e. half a Rabi oscillation, with frequency ω and $\Gamma = 0$, preceded and followed by two short pulses of area $\pi/4$. The

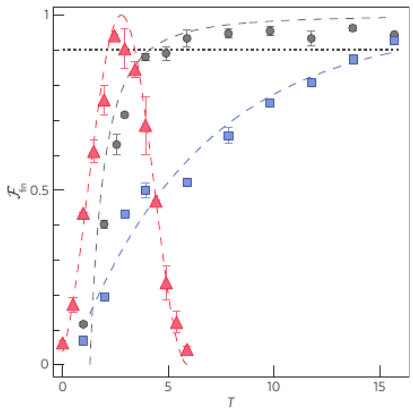

Figure 1.2: Fidelity of the final state as a function of the duration for the composite pulse protocol (red triangles), the RC protocol (grey circles) and the LZ protocol (blue squares). The dashed lines are numerical predictions. Reproduced from Ref. [13].

π-pulse corresponds to a time

$$T_\pi \omega = \pi. \tag{1.29}$$

This values represents the quantum speed limit discussed in Ref. [13]. In Fig. 1.2 is plotted the fidelity of the composite pulse protocol (together with the fidelity of other two protocols) as a function of the duration. It is clear that, while the composite pulse protocol minimizes the time of the transfer, it is not a robust method to variation in the parameter T.

CHAPTER 2

Overview of the STIRAP process

The simplest STIRAP scheme involves three non-degenerate states coupled by two coherent radiation fields: the *pump pulse*, which couples the initial populated state $|1\rangle$ and the intermediate state $|2\rangle$, and the *Stokes pulse*, witch couples the intermediate state with the final state $|3\rangle$. The essential ingredients are the efficiency of the $|1\rangle - |3\rangle$ transfer on the basis of the counter-intuitive order of the laser pulses (there must be an overlap between them) and the related evolution of the eigenstates of the time-dependent Hamiltonian.

When coherent radiation is applied, the Hamiltonian of the matter-field system as a

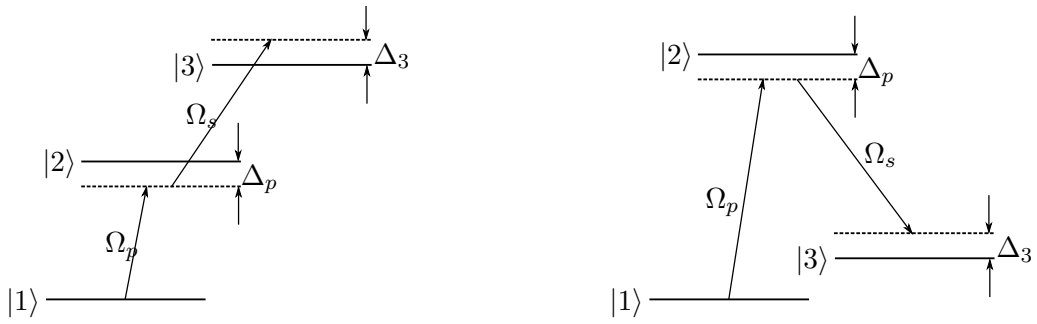

(a) Ladder level configuration. **(b)** Λ level configuration.

Figure 2.1: Level schemes of three-level systems.

whole includes both atomic-excitation energy and field-interaction energy; its eigenstates, which include in some manner the unperturbed, bare states of the atom, and the interaction with the two radiation fields, are called the *dressed states*. As the Hamiltonian changes in time with varying lasers' intensities, the instantaneous dressed states change in time. The photon numbers are not taken into account, and the term *adiabatic states* is used to refer to such time-varying dressed states (i.e., the instantaneous eigenstates of

the Hamiltonian). The adiabatic theorem [17] states that if an Hamiltonian changes in time sufficiently slow, the system remains at all times in one adiabatic state.

The unperturbed, bare states of the atom are $|1\rangle$, $|2\rangle$ and $|3\rangle$; initially state $|1\rangle$

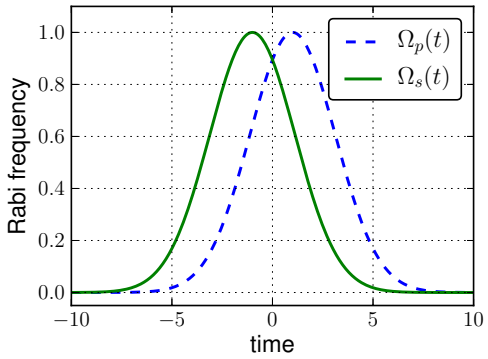

(a) Gaussian Rabi frequencies as functions of time.

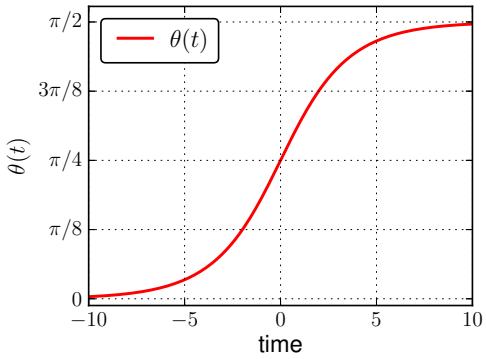

(b) The resulting $\theta(t) = \arctan[\Omega_p(t)/\Omega_s(t)]$ from 2.2a.

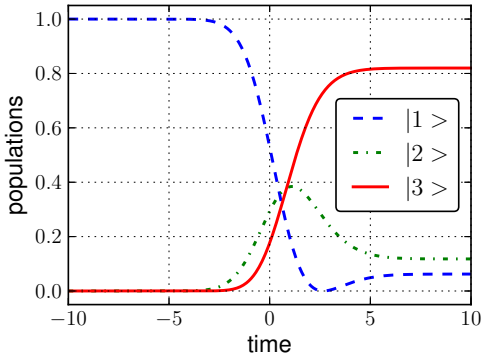

(c) Populations evolution.

Figure 2.2: Counter-intuitive STIRAP pulse sequence, with Gaussian pulses, for transfer from initial $|1\rangle$ to final $|3\rangle$ states. Time and Rabi frequencies are in arbitrary units.

is populated while the other states are empty. In the counter-intuitive pulse scheme, see Fig. 2.2a, the Stokes laser, Rabi frequency Ω_s, arrives first and couples two empty states. However, this does not mean that it has no effect; in fact, the Stokes laser creates a coherent superposition of the two unpopulated states $|2\rangle$ and $|3\rangle$. Then, the pump laser, Rabi frequency Ω_p, arrives and couples this coherent superposition with the populated state $|1\rangle$. The pulsed nature of the interaction between the laser light and the atoms or molecules can be produced either by causing the particles to traverse overlapping continuous-wave laser beams or by illuminating essentially stationary particles with pulsed lasers.

If two-photon resonance between initial and final states applies, a *dark state* [19] is formed. A dark state (for a review on dark states see [20]) is defined as a state from which the applied lasers cannot transfer population to the intermediate state $|2\rangle$. It turns out that this dark state is an adiabatic state, thus, if the Hamiltonian is slowly changing and this state is initially populated, the system remains at all times in this state and no population is transferred to state $|2\rangle$. Rather, it is possible to make this state coincide with state $|1\rangle$ at the begin of the process and with state $|3\rangle$ at the end of the process. Thus all the population is directly channelled from state $|1\rangle$ into state $|3\rangle$. For a review of the STIRAP process see [4].

2.1 The STIRAP Hamiltonian

The Hamiltonian within the rotating wave approximation (RWA, [5, 21]) in bare-atom basis reads as in the following:

$$H_0(t) = \frac{\hbar}{2}\begin{pmatrix} 0 & \Omega_p(t) & 0 \\ \Omega_p(t) & 2\Delta_p & \Omega_s(t) \\ 0 & \Omega_s(t) & 2\Delta_3 \end{pmatrix}. \tag{2.1}$$

The phases are chosen so that the Hamiltonian is Real. The interaction between the pump and Stokes fields (with carrier frequencies ω_p and ω_s respectively) and the system is determined by the Rabi frequencies $\Omega_p(t)$ and $\Omega_s(t)$, which must be ordered counter-intuitively

$$\lim_{t\to t_i}\frac{\Omega_p(t)}{\Omega_s(t)} = 0 \qquad\qquad \lim_{t\to t_f}\frac{\Omega_s(t)}{\Omega_p(t)} = 0 \tag{2.2}$$

i.e. the Stokes laser acts first (the pump laser is turned off at t_i) and the pump laser acts last (the Stokes laser is turned off at t_f).

The detunings from resonance are defined by

$$\begin{aligned} \Delta_p &= \omega_p - \frac{E_2 - E_1}{\hbar}, \\ \Delta_s &= \omega_s - \frac{|E_3 - E_2|}{\hbar}, \\ \Delta_3 &= \begin{cases} \Delta_p + \Delta_s, & \text{ladder configuration,} \\ \Delta_p - \Delta_s, & \Lambda \text{ configuration.} \end{cases} \end{aligned} \tag{2.3}$$

where E_1, E_2 and E_3 are the energies of the bare states of the atom. In STIRAP the Rabi frequencies are time-varying and the detunings are fixed. The conditions for the resonances are

- two-photon resonance: $\Delta_3 = \Delta_p \pm \Delta_s = 0$ (see Fig. 2.3),
- one-photon resonance: $\Delta_p = \Delta_s = \Delta_3 = 0$.

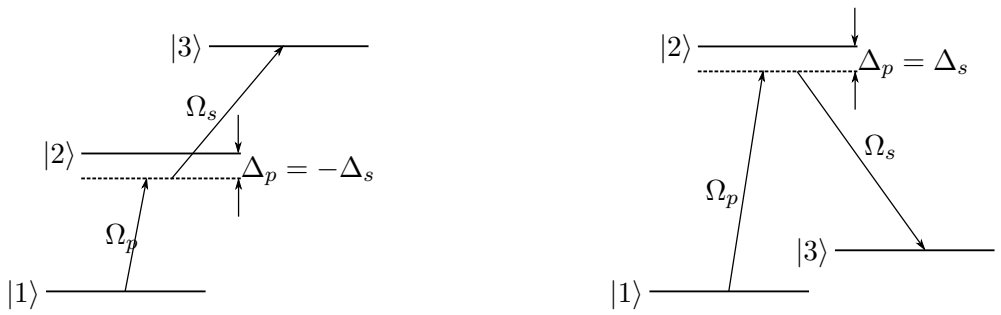

(a) Ladder level configuration.

(b) Λ level configuration.

Figure 2.3: Level schemes of STIRAP for the two-photon resonance condition $\Delta_3 = 0$.

Although the presence of single-photon detunings does not prevent population transfer, it is essential that the two-photon resonance condition $\Delta_3 = 0$ apply (for a discussion of the two-photon linewidth in Λ system see [22]).

It is useful to define an effective Rabi frequency Ω_0

$$\Omega_0(t)^2 = \Omega_p(t)^2 + \Omega_s(t)^2. \tag{2.4}$$

Within the required condition of two-photon resonance the Hamiltonian of Eq. (2.1) becomes

$$H_0(t) = \frac{\hbar}{2} \begin{pmatrix} 0 & \Omega_p(t) & 0 \\ \Omega_p(t) & 2\Delta_p & \Omega_s(t) \\ 0 & \Omega_s(t) & 0 \end{pmatrix}. \tag{2.5}$$

The instantaneous eigenvalues of this matrix are

$$\begin{aligned} \lambda_1(t) &= \lambda_0(t) = 0 \\ \lambda_2(t) &= \lambda_-(t) = \frac{\hbar}{2}\left(\Delta_p - \sqrt{\Delta_p^2 + \Omega_0(t)^2}\right) \\ \lambda_3(t) &= \lambda_+(t) = \frac{\hbar}{2}\left(\Delta_p + \sqrt{\Delta_p^2 + \Omega_0(t)^2}\right) \end{aligned} \tag{2.6}$$

and the normalized instantaneous eigenvectors (adiabatic states) are

$$|a_0(t)\rangle = \frac{1}{\Omega_0(t)} \begin{pmatrix} \Omega_s(t) \\ 0 \\ -\Omega_p(t) \end{pmatrix}, \qquad |a_n(t)\rangle = \frac{1}{\sqrt{4\lambda_n(t)^2 + \Omega_0(t)^2}} \begin{pmatrix} \Omega_p(t) \\ 2\lambda_n(t) \\ \Omega_s(t) \end{pmatrix} \quad \text{for } n = -, + \tag{2.7}$$

This solution can be written in a simpler form defining

$$\begin{aligned}\tan\theta(t) &= \frac{\Omega_p(t)}{\Omega_s(t)},\\ \tan\phi(t) &= \frac{\Omega_0(t)}{\Delta_p + \sqrt{\Delta_p^2 + \Omega_0(t)^2}}.\end{aligned} \tag{2.8}$$

Indeed the eigenvalues can be written as

$$\begin{aligned}\lambda_1(t) &= \lambda_0(t) = 0\\ \lambda_2(t) &= \lambda_-(t) = -\frac{\hbar}{2}\Omega_0(t)\tan\phi(t)\\ \lambda_3(t) &= \lambda_+(t) = \frac{\hbar}{2}\Omega_0(t)\cot\phi(t)\end{aligned} \tag{2.9}$$

and the instantaneous eigenvectors (see [5, 23])

$$|a_0(t)\rangle = \begin{pmatrix}\cos\theta(t)\\ 0\\ -\sin\theta(t)\end{pmatrix}, \quad |a_-(t)\rangle = \begin{pmatrix}\sin\theta(t)\cos\phi(t)\\ -\sin\phi(t)\\ \cos\theta(t)\cos\phi(t)\end{pmatrix}, \quad |a_+(t)\rangle = \begin{pmatrix}\sin\theta(t)\sin\phi(t)\\ \cos\phi(t)\\ \cos\theta(t)\sin\phi(t)\end{pmatrix}. \tag{2.10}$$

The solution without the condition of two-photon resonance is reported in ref. [23].

2.2 Dark State and Evolution

The state $|a_0(t)\rangle$ is a dark state, its projection on $|2\rangle$ being zero at all times

$$\langle a_0(t)|2\rangle = 0 \quad \forall\, t. \tag{2.11}$$

Notice that if the pulse sequence is counter-intuitive i.e. it follows the time-dependence of Eq. (2.2)

$$\lim_{t\to t_i}\frac{\Omega_p(t)}{\Omega_s(t)} = 0 \qquad \lim_{t\to t_f}\frac{\Omega_s(t)}{\Omega_p(t)} = 0 \tag{2.2}$$

then

$$\lim_{t\to t_i}\tan\theta(t) = 0 \quad \lim_{t\to t_f}\tan\theta(t) = +\infty. \tag{2.12a}$$

Assuming $\Omega_p(t), \Omega_s(t) > 0$, this imply that

$$\lim_{t\to t_i}\theta(t) = 0 \quad \lim_{t\to t_f}\theta(t) = \frac{\pi}{2}. \tag{2.12b}$$

Therefore $\theta(t)$ varies from 0 at the initial time to $\frac{\pi}{2}$ at the final time. The dark state $|a_o(t)\rangle$ then varies from $|1\rangle$ to $|3\rangle$

$$|a_0(t_i)\rangle = \begin{pmatrix}1\\ 0\\ 0\end{pmatrix} = |1\rangle \quad \text{and} \quad |a_0(t_f)\rangle = \begin{pmatrix}0\\ 0\\ -1\end{pmatrix} = -|3\rangle.$$

If the evolution is adiabatic, and the state $|a_o(t)\rangle$ is initially populated, then all population is directly channeled from state $|1\rangle$ into state $|3\rangle$ and no population is found in state $|2\rangle$ during the process. Fig. 2.2 reports for a counter-intuitive pulse sequence an example of the temporal evolution for Rabi frequencies Ω_p and Ω_s, $\theta(t)$ and populations.

2.3 Condition for Adiabatic Following

The adiabatic theorem [17] states that if an Hamiltonian changes in time sufficiently slow and at the initial time the system starts in an instantaneous eigenstate (adiabatic state) of that Hamiltonian and if that state remains non-degenerate, then the system will remain at all times in that adiabatic state. This means that the state vector $|\psi(t)\rangle$ solution of the Schrödinger equation

$$\mathrm{i}\hbar\frac{\partial}{\partial t}|\psi(t)\rangle = H_0(t)\,|\psi(t)\rangle \tag{2.13}$$

will adiabatically follow that adiabatic state. As pointed out in the preceding section the interesting adiabatic state for STIRAP is the dark state $|a_0(t)\rangle$, so:

$$|\psi(t)\rangle \simeq e^{\mathrm{i}\varphi(t)}\,|a_0(t)\rangle \quad \forall\, t. \tag{2.14}$$

In order to derive the condition for which the Hamiltonian change in time may be considered slow it is necessary to impose that the transitions between $|a_0(t)\rangle$ and the others adiabatic states $|a_\pm(t)\rangle$ is small during all the evolution (Ref. [18] and Sec. 1.1.2). That is

$$|\langle a_\pm(t)|\dot{a}_0(t)\rangle| \ll \frac{|\lambda_\pm - \lambda_0|}{\hbar}. \tag{2.15}$$

Using Eqs. (2.10) and (2.6) we find ([5, 24])

$$\left|\dot{\theta}(t)\right| \ll \left|\frac{1}{2}\left(\Delta_p - \sqrt{\Delta_p^2 + \Omega_p(t)^2 + \Omega_s(t)^2}\right)\right| \tag{2.16a}$$

and

$$\dot{\theta}(t) = \frac{\dot{\Omega}_p(t)\Omega_s(t) - \Omega_p(t)\dot{\Omega}_s(t)}{\Omega_p(t)^2 + \Omega_s(t)^2}. \tag{2.16b}$$

We may consider Eq. (2.16a) as a "local" adiabaticity condition, because it can be evaluated at any instant of time. This condition must be valid all throughout the interaction for the evolution to be really adiabatic. It is important to notice that $\dot{\theta}(t)$ cannot be zero for all the time of the evolution, in fact this would imply the pulses to be simultaneous

$$\begin{aligned} &\dot{\theta}(t) = 0 \quad \Rightarrow \quad \dot{\Omega}_p(t)\Omega_s(t) - \Omega_p(t)\dot{\Omega}_s(t) = 0 \\ &\Rightarrow \quad \frac{\dot{\Omega}_p(t)}{\Omega_p(t)} = \frac{\dot{\Omega}_s(t)}{\Omega_s(t)} \quad \Rightarrow \quad \Omega_p(t) = C\cdot\Omega_s(t) \end{aligned} \tag{2.17}$$

where C is an arbitrary constant independent of time. Simultaneous pulses do not fulfill the STIRAP requirement of Eq. (2.2) of counter-intuitive laser pulses.

A "global" adiabaticity condition may be derived from Eq. (2.16) by time averaging both side of the equation and assuming $\Delta_p(t) \ll \Omega_p(t), \Omega_s(t)$

$$\frac{1}{\tau}\int_{t_i}^{t_f} \dot{\theta}(t)dt \ll \frac{1}{\tau}\int_{t_i}^{t_f} \sqrt{\Omega_p(t)^2 + \Omega_s(t)^2}dt \tag{2.18a}$$

$$\Rightarrow \frac{\pi}{2\tau} \ll \Omega_{eff}(t) \tag{2.18b}$$

$$\Rightarrow \Omega_{eff}(t)\tau \gg 1 \tag{2.18c}$$

where

$$\Omega_{eff} = \frac{1}{\tau}\int_{t_i}^{t_f} \sqrt{\Omega_p(t)^2 + \Omega_s(t)^2}dt = \frac{1}{\tau}\int_{t_i}^{t_f} \Omega_0(t)dt. \tag{2.18d}$$

Here τ is the characteristic time of the transfer, given by the interval of time where $\Omega_p(t)$ and $\Omega_p(t)$ overlap. Numerical simulation studies and ref. [5] give as qualitative estimation for the "global" adiabaticity condition

$$\Omega_{eff}\tau > 10 \tag{2.19}$$

Typical STIRAP pulses are written as

$$\begin{aligned} \Omega_p(t) &= Af(\frac{t-\tau}{T}) \\ \Omega_s(t) &= Af(\frac{t+\tau}{T}) \end{aligned} \tag{2.20}$$

where $f(t)$ is a pulse envelope of unit maximum value and A is the maximum Rabi Frequency. The "global" qualitative condition may then be written as

$$A\tau > 20. \tag{2.21}$$

For a comparison with the experimental conditions, it is important to write the above condition in terms of quantities as $A/2\pi$ measured in MHz and time measured in μs

$$\frac{A}{2\pi}\tau > 3.18. \tag{2.22}$$

It is interesting to study this condition more "quantitatively" when interested in minimizing the time of the transfer. In fact, the constant on the r.h.s. of Eq. (2.21), given the time τ during with we want the transfer to be almost complete and the Rabi frequency maximum A, depends on the pulse shape $f(t)$. This lead to understand what is the shape that minimize the time of the transfer given the maximum Rabi frequency reachable. This will be examined in more detail in section 4.8.

CHAPTER 3

Super-Adiabatic STIRAP

It is interesting to apply the theory described in section 1.2 to the STIRAP. With that theory we obtain the super-adiabatic correction $H_1(t)$ to the STIRAP Hamiltonian $H_0(t)$ and we can apply to the system the total Hamiltonian $H(t) = H_0(t) + H_1(t)$.

If the total Hamiltonian $H(t)$ is applied to the system, the evolution will follow exactly the instantaneous eigenstates of the STIRAP Hamiltonian, also if the condition for the adiabatic following (2.16) is not satisfied. If the system starts in the dark state $|a_0(t_i)\rangle = |1\rangle$, then it will remain in that dark state for all the evolution. The transition amplitudes to other states $|a^{\pm}(t)\rangle$ are exactly zero, and at the end of the process all the population will be in state $|a(t_f)\rangle = |3\rangle$ with exactly zero population in state $|2\rangle$ for all the time of the process. This because $|a_0(t)\rangle$ is a dark state, i.e. $\langle a_0(t)|2\rangle = 0,\ \forall t$.

It is interesting that the adiabatic following of eigenstates of $H_0(t)$ will happen for any choice of the parameters that characterize the STIRAP "slowness". With reference to Eq. (2.20) these are A and τ. So it is possible to achieve a super-adiabatic evolution even if $A \to 0$, i.e. with very small values of the applied pump and Stoke fields, and even with $\tau \to 0^+$, i.e. in arbitrary short time. The parameter τ cannot be zero because it is needed that the pulses are counter-intuitively ordered.

3.1 The Super-Adiabatic STIRAP Hamiltonian

Recall that the Three-level Hamiltonian under two-photon resonance is

$$H_0(t) = \frac{\hbar}{2}\begin{pmatrix} 0 & \Omega_p(t) & 0 \\ \Omega_p(t) & 2\Delta_p(t) & \Omega_s(t) \\ 0 & \Omega_s(t) & 0 \end{pmatrix}. \tag{3.1}$$

The phases can be chosen such that the Hamiltonian is Real. In order to be more general we let the possibility to the one-photon detuning $\Delta_p(t)$ to be variable in time.

Our purpose is to obtain the super-adiabatic correction to STIRAP defined in Eq. (1.19). To calculate $H_1(t)$ we need the instantaneous eigenstates of $H_0(t)$ calculated in section 2.1 (Eqs. (2.7) and (2.10)).

Using Eq. (1.19) with $\{|n(t)\rangle\}_n = \{|a_0(t)\rangle, |a_-(t)\rangle, |a_+(t)\rangle\}$ we get

$$H_1(t) = \mathrm{i}\hbar \begin{pmatrix} 0 & \dot{\phi}(t)\sin\theta(t) & \dot{\theta}(t) \\ -\dot{\phi}(t)\sin\theta(t) & 0 & -\dot{\phi}(t)\cos\theta(t) \\ -\dot{\theta}(t) & \dot{\phi}(t)\cos\theta(t) & 0 \end{pmatrix} \tag{3.2}$$

It is useful to give the matrix elements above as a function of the Rabi frequencies $\Omega_s(t)$ and $\Omega_p(t)$ and the one-photon detuning $\Delta_p(t)$. We get

$$\begin{aligned} H_1(t)_{13} &= \mathrm{i}\hbar \frac{\dot{\Omega}_p(t)\Omega_s(t) - \Omega_p(t)\dot{\Omega}_s(t)}{\Omega_p(t)^2 + \Omega_s(t)^2} = \\ &= \mathrm{i}\hbar \frac{\dot{\Omega}_p(t)\Omega_s(t) - \Omega_p(t)\dot{\Omega}_s(t)}{\Omega_0(t)^2} \equiv \mathrm{i}\hbar \frac{\Omega_d(t)}{2} \end{aligned} \tag{3.3a}$$

where the last equality defines Ω_d as $\Omega_d(t) = 2\dot{\theta}(t)$.

$$\begin{aligned} H_1(t)_{12} &= -\mathrm{i}\hbar \frac{\Omega_p\left(\dot{\Delta}_p\left(\Omega_p^2 + \Omega_s^2\right) - \Delta_p\left(\Omega_p\dot{\Omega}_p + \Omega_s\dot{\Omega}_s\right)\right)}{2\left(\Omega_p^2 + \Omega_s^2\right)\left(\Delta_p^2 + \Omega_p^2 + \Omega_s^2\right)} \\ &= -\mathrm{i}\hbar \frac{\Omega_p\left(\dot{\Delta}_p\Omega_0 - \Delta_p\dot{\Omega}_0\right)}{2\Omega_0\left(\Delta_p^2 + \Omega_0^2\right)} \end{aligned} \tag{3.3b}$$

$$\begin{aligned} H_1(t)_{23} &= \mathrm{i}\hbar \frac{\Omega_s\left(\dot{\Delta}_p\left(\Omega_p^2 + \Omega_s^2\right) - \Delta_p\left(\Omega_p\dot{\Omega}_p + \Omega_s\dot{\Omega}_s\right)\right)}{2\left(\Omega_p^2 + \Omega_s^2\right)\left(\Delta_p^2 + \Omega_p^2 + \Omega_s^2\right)} \\ &= \mathrm{i}\hbar \frac{\Omega_s\left(\dot{\Delta}_p\Omega_0 - \Delta_p\dot{\Omega}_0\right)}{2\Omega_0\left(\Delta_p^2 + \Omega_0^2\right)} \end{aligned} \tag{3.3c}$$

$$H_1(t)_{ij} = H_1(t)^*_{ji} \tag{3.3d}$$

Notice that

$$H_1(t)_{12} = -\frac{\Omega_p(t)}{\Omega_s(t)} H_1(t)_{23}. \tag{3.4}$$

The dependence of Ω_p, Ω_s, Ω_0 and Δ_p on t is determines the super-adiabatic correction. The super-adiabatic correction $H_1(t)$ is purely imaginary because of the initial choice of phases (that have been chosen for the STIRAP Hamiltonian $H_0(t)$ to be Real). This solution is in agreement with equation (5) of ref. [25] in which the condition $\dot{\Delta}_p(t) = 0$ is imposed.

The total Hamiltonian $H(t) = H_0(t) + H_1(t)$ is then

$$H(t) = \frac{\hbar}{2} \begin{pmatrix} 0 & \Omega_p + \mathrm{i}2\dot{\phi}\sin\theta & \mathrm{i}2\dot{\theta} \\ \Omega_p - \mathrm{i}2\dot{\phi}\sin\theta & 2\Delta_p & \Omega_s - \mathrm{i}2\dot{\phi}\cos\theta \\ -\mathrm{i}2\dot{\theta} & \Omega_s + \mathrm{i}2\dot{\phi}\cos\theta & 0 \end{pmatrix} \tag{3.5}$$

with all quantities depending on t.

It is important to understand the role of each matrix element of the super-adiabatic hamiltonian and how it can be applied to a system.

In Fig. 3.1 are represented some numerical simulation of the population evolution with the STIRAP and with the super-adiabatic STIRAP.

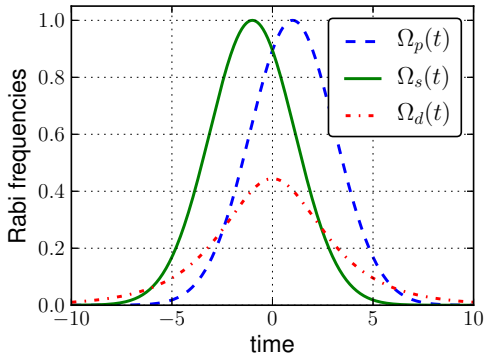

(a) Gaussian Rabi frequencies and the detuning pulse $\Omega_d(t)$ as functions of time.

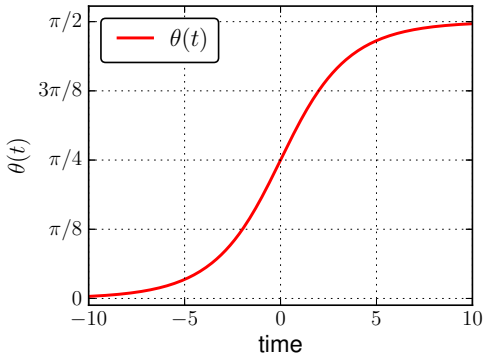

(b) The resulting $\theta(t) = \arctan\left[\Omega_p(t)/\Omega_s(t)\right]$ from (a).

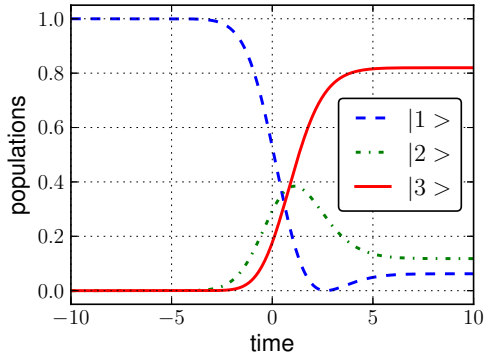

(c) Populations evolution for simple STIRAP.

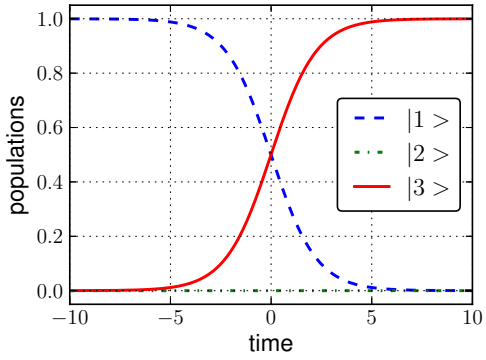

(d) Populations evolution for Super-Adiabatic STIRAP.

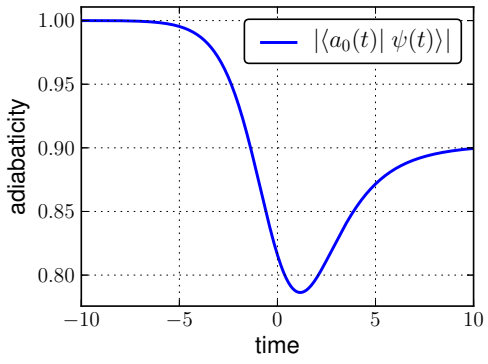

(e) Adiabatic following for simple STIRAP.

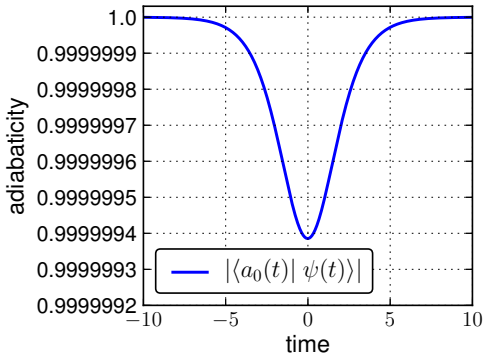

(f) Adiabatic following for Super-Adiabatic STIRAP.

Figure 3.1: Comparison of the simple STIRAP evolution against Super-Adiabatic STIRAP evolution. Time and Rabi frequencies are in arbitrary units. Notice the scale in Fig. (f): the difference from 1 in the adiabaticity is of the order of 10^{-6} and is due to numerical errors in the simulation.

3.1.1 Matrix Elements $H_1(t)_{12}$ and $H_1(t)_{23}$

Matrix element $H_1(t)_{12}$ couple the initial state $|1\rangle$ with the intermediate state $|2\rangle$, $H_1(t)_{23}$ couple the intermediate state with the final state $|3\rangle$. These corrections represent an addition to the pump and Stokes pulses. They influence the system evolution by modifying the lasers pulses operating in the STIRAP: they add a phase relation between $\Omega_p(t)$ and $\Omega_s(t)$, and they modify their temporal dependence.

These matrix elements can vanish for a proper choice of $\Delta_p(t)$. Recall that the matrix elements are

$$H_1(t)_{12} = \mathrm{i}\hbar\dot{\phi}(t)\sin\theta(t) = \mathrm{i}\hbar\frac{\Omega_p\left(\dot{\Omega}_0\Delta_p - \Omega_0\dot{\Delta}_p\right)}{2\Omega_0\left(\Delta_p^2+\Omega_0^2\right)} \tag{3.6a}$$

$$H_1(t)_{23} = -\mathrm{i}\hbar\dot{\phi}(t)\cos\theta(t) = -\mathrm{i}\hbar\frac{\Omega_s\left(\dot{\Omega}_0\Delta_p - \Omega_0\dot{\Delta}_p\right)}{2\Omega_0\left(\Delta_p^2+\Omega_0^2\right)}. \tag{3.6b}$$

and that

$$\sin\theta(t) = \frac{\Omega_p(t)}{\Omega_0(t)}, \quad \cos\theta(t) = \frac{\Omega_s(t)}{\Omega_0(t)} \tag{3.7a}$$

$$\dot{\phi}(t) = \frac{\dot{\Omega}_0(t)\Delta_p(t) - \Omega_0(t)\dot{\Delta}_p(t)}{2\left(\Delta_p(t)^2+\Omega_0(t)^2\right)}. \tag{3.7b}$$

These matrix elements are identically zero in the trivial case $\Omega_p(t) = \Omega_s(t) = \Omega_0(t) = 0$, $\Delta_p(t) \neq 0$; or in the more interesting case in which $\Delta_p(t)$ is proportional to $\Omega_0(t) \neq 0$ ($\dot{\phi}(t) = 0$)

$$\begin{aligned} \Delta_p(t) = C\cdot\Omega_0(t) \quad &\Rightarrow \quad \frac{\dot{\Delta}_p(t)}{\Delta_p(t)} = \frac{\dot{\Omega}_0(t)}{\Omega_0(t)} \\ &\Rightarrow \quad \dot{\Delta}_p(t)\Omega_0(t) - \Delta_p(t)\dot{\Omega}_0(t) = 0 \\ &\Rightarrow \quad H_1(t)_{12} = H_1(t)_{23} = 0. \end{aligned} \tag{3.8}$$

The mathematical structure of last equation is similar to that of Eq. (2.17). Notice that Eq. (3.8) is also valid for $C = 0$, i.e., $\Delta_p(t)$ being a constant equal to zero.

3.1.2 Matrix Element $H_1(t)_{13}$

Matrix element $H_1(t)_{13}$ is the most interesting one because it couples directly the initial and the final state. It is

$$H_1(t)_{13} = \mathrm{i}\hbar\dot{\theta}(t) = \mathrm{i}\hbar\frac{\dot{\Omega}_p(t)\Omega_s(t) - \Omega_p(t)\dot{\Omega}_s(t)}{\Omega_p(t)^2+\Omega_s(t)^2} \equiv \mathrm{i}\hbar\frac{\Omega_d(t)}{2}. \tag{3.9}$$

having defined the *detuning pulse*

$$\Omega_d(t) \equiv 2\dot{\theta}(t). \tag{3.10}$$

This definition was introduced in Refs.[26] and [27] by noting that in the basis of the $|a_n(t)\rangle$ eigenstates, with $|a_0(t)\rangle$ the dark state, $\Omega_d(t)$ appears as a detuning term along the diagonal.

If a proper time dependence of $\Omega_p(t)$ and $\Omega_s(t)$ can be found such that the detuning pulse (and then $H_1(t)_{13}$) is identically zero for all the evolution time, than the super-adiabatic transfer could be achieved without any direct coupling of the initial and final states. This means that, by eventually changing only the shape and/or the phase of the pump and Stokes fields, a super-adiabatic evolution of the system could be reached. But this is not the case. In fact as demonstrated in Eq.(2.17)

$$H_1(t)_{13} = 0 \quad \Rightarrow \quad \dot{\theta}(t) = 0 \quad \Rightarrow \quad \Omega_p(t) \propto \Omega_s(t) \tag{3.11}$$

and then condition (2.2) is not fulfilled, which means that the pulse sequence is not counter-intuitive. This imply that Eqs. (2.12)

$$\lim_{t\to t_i} \tan\theta(t) = 0 \quad \lim_{t\to t_f} \tan\theta(t) = +\infty \tag{2.12a}$$

$$\lim_{t\to t_i} \theta(t) = 0 \quad \lim_{t\to t_f} \theta(t) = \frac{\pi}{2} \tag{2.12b}$$

do not hold anymore and then the dark state $|a_0(t)\rangle$ does not link the state $|1\rangle$ with the state $|3\rangle$.

The selection rules for electric dipole transition require that states which are linked have different parity. The pump laser links state $|1\rangle$ and state $|2\rangle$ so they have different parity, the same for states $|2\rangle$ and $|3\rangle$ which are linked by the Stokes laser, so the initial and final states for STIRAP are required to have equal parity. The matrix element $H(t)_{13} \propto \Omega_d(t)$ links directly state $|1\rangle$ with state $|3\rangle$. This interaction cannot occur with a one-photon dipole transition but it can take place with a magnetic dipole transition or with a two-photon transition.

3.2 The Detuning Pulse $\Omega_d(t)$

In Sec. 3.1.2 we have established that the detuning pulse $\Omega_d(t)$ is a required interaction and cannot be zero for the super-adiabatic evolution. Now we analyze it in more detail.

Assume that $\Delta_p(t) \propto \Omega_0(t)$ so that the matrix elements $H_1(t)_{12}$ and $H_1(t)_{23}$ became identically zero. The super-adiabatic Hamiltonian then is

$$H(t) = \frac{\hbar}{2}\begin{pmatrix} 0 & \Omega_p(t) & \mathrm{i}\Omega_d(t) \\ \Omega_p(t) & 2\Delta_p(t) & \Omega_s(t) \\ -\mathrm{i}\Omega_d(t) & \Omega_s(t) & 0 \end{pmatrix} \tag{3.12}$$

and remember that

$$\Omega_d(t) = 2\dot{\theta}(t) = 2\frac{\dot{\Omega}_p(t)\Omega_s(t) - \Omega_p(t)\dot{\Omega}_s(t)}{\Omega_p(t)^2 + \Omega_s(t)^2} \tag{3.13}$$

and that $\Omega_p(t)$, $\Omega_s(t)$ and then $\Omega_d(t)$ are all Real quantities. As represented in Fig. 3.2 $\Omega_d(t)$ represents a direct coupling between state $|1\rangle$ and $|3\rangle$.

In the following subsections we analyze the properties of the detuning pulse.

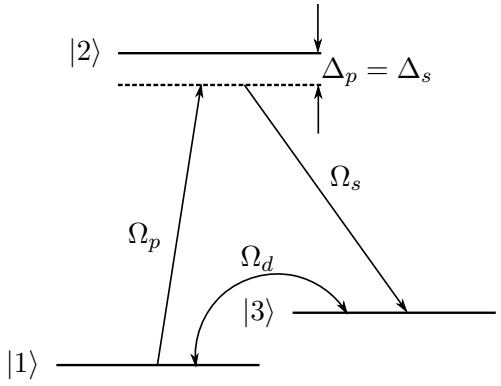

Figure 3.2: Λ system with the new interaction $\Omega_d(t)$.

3.2.1 The Detuning Pulse as a π-pulse

First of all notice that $\Omega_d(t)$ is a π-pulse

$$\int_{t_i}^{t_f} \Omega_d(t)dt = \int_{t_i}^{t_f} 2\dot{\theta}(t)dt = 2\left[\theta(t_f) - \theta(t_i)\right] = 2\left[\frac{\pi}{2} - 0\right] = \pi. \tag{3.14}$$

A π pulse connecting state $|1\rangle$ and $|3\rangle$ will produce complete population transfer. A π pulse is not a robust method in fact it takes advantage of the Rabi oscillations and if the area of that pulse is not exactly π no complete transfer is achieved, see Sec. 1.3.

Fig. 3.3 reports the Rabi oscillations between state $|1\rangle$ and $|3\rangle$ supposing that $\Omega_p(t) = \Omega_s(t) = 0$ and only $\Omega_d(t)$ is applied, for instance through a radio-frequency/microwave field: the population oscillate between the states coupled by the interaction. All the population occupies the state $|3\rangle$ only if the area of the pulse is an odd multiple of π

$$A(t) = \int_{t_i}^{t} \Omega_d(t')dt' = (2n+1)\,\pi, \quad \text{for } n = 0, 1, 2\ldots \tag{3.15}$$

For a super-adiabatic evolution $\Omega_d(t)$ must have exactly the shape that results from Eq. (3.13).

These constraints are much stronger then the adiabatic condition. However, it is not necessary that Eq. (3.13) be exactly valid to obtain improvement of STIRAP, as will be confirmed by numerical results shown below. Moreover we will see that the STIRAP pulses make the π pulse more robust.

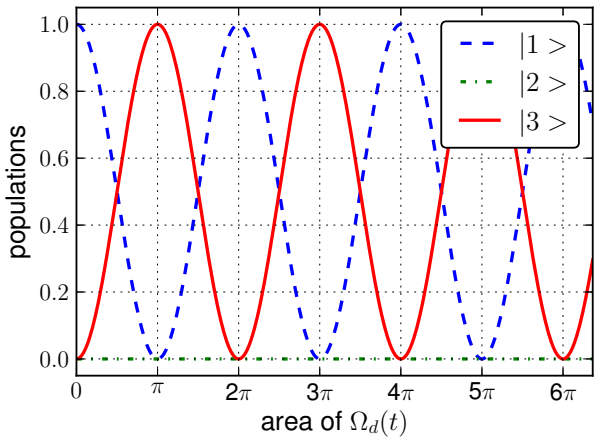

Figure 3.3: Rabi oscillations if only pulse $\Omega_d(t)$ is applied. Every time the area of the pulse is augmented by π there is a complete inversion of population between the states $|1\rangle$ and $|3\rangle$. To obtain all population being in state $|3\rangle$ the pulse area has to be exactly an odd multiple of π.

It is worth noting that the same result was reached by Unanyan et al. [26] in 1997 without using the super-adiabatic approach and searching for an improvement of the STIRAP efficiency by adding another low frequency field.

3.2.2 Phase of the Detuning Pulse

In the basis set used to obtain real elements of the STIRAP Hamiltonian, the matrix element $H(t)_{13} \propto \mathrm{i}\Omega_d(t)$ is a pure imaginary quantity.

To understand what does this mean we drop the conditions on the basis that make the pump and Stokes Rabi frequencies Real. We see how definition of $H_1(t)$ changes in the more general (but equivalent) case in which these Rabi frequencies can be complex functions of time.

The STIRAP Hamiltonian then reads [21]

$$H_0(t) = \frac{\hbar}{2}\begin{pmatrix} 0 & \Omega_p^*(t) & 0 \\ \Omega_p(t) & 2\Delta_p(t) & \Omega_s^*(t) \\ 0 & \Omega_s(t) & 0 \end{pmatrix} \quad \text{for the Ladder level scheme} \tag{3.16a}$$

$$H_0(t) = \frac{\hbar}{2}\begin{pmatrix} 0 & \Omega_p^*(t) & 0 \\ \Omega_p(t) & 2\Delta_p(t) & \Omega_s(t) \\ 0 & \Omega_s^*(t) & 0 \end{pmatrix} \quad \text{for the } \Lambda \text{ level scheme} \tag{3.16b}$$

and the super-adiabatic one, with the condition on $\Delta_p(t)$ to make $H_1(t)_{12}$ and $H_1(t)_{23}$

identically zero, reads

$$H_0(t) = \frac{\hbar}{2}\begin{pmatrix} 0 & \Omega_p^*(t) & \Omega_d(t) \\ \Omega_p(t) & 2\Delta_p(t) & \Omega_s^*(t) \\ \Omega_d^*(t) & \Omega_s(t) & 0 \end{pmatrix} \quad \text{for the Ladder level scheme} \tag{3.17a}$$

$$H_0(t) = \frac{\hbar}{2}\begin{pmatrix} 0 & \Omega_p^*(t) & \Omega_d(t) \\ \Omega_p(t) & 2\Delta_p(t) & \Omega_s(t) \\ \Omega_d^*(t) & \Omega_s^*(t) & 0 \end{pmatrix} \quad \text{for the } \Lambda \text{ level scheme} \tag{3.17b}$$

where

$$\Omega_d(t) = \mathrm{i}2\frac{\dot{\Omega}_p^*(t)\Omega_s^*(t) - \Omega_p^*(t)\dot{\Omega}_s^*(t)}{|\Omega_p(t)|^2 + |\Omega_s(t)|^2} \quad \text{for the Ladder level scheme} \tag{3.18a}$$

$$\Omega_d(t) = \mathrm{i}2\frac{\dot{\Omega}_p^*(t)\Omega_s(t) - \Omega_p^*(t)\dot{\Omega}_s(t)}{|\Omega_p(t)|^2 + |\Omega_s(t)|^2} \quad \text{for the } \Lambda \text{ level scheme} \tag{3.18b}$$

is a more general definition of the detuning pulse of that given in Eq. (3.13).

If we write

$$\begin{aligned} \Omega_p(t) &= e^{i\phi_p}\,|\Omega_p(t)| \\ \Omega_s(t) &= e^{i\phi_s}\,|\Omega_s(t)| \\ \Omega_d(t) &= e^{i\phi_d}\,|\Omega_d(t)| \end{aligned} \tag{3.19}$$

the super-adiabatic condition of Eqs. (3.18) requires

$$\phi_d = \frac{\pi}{2} - \phi_p - \phi_s \quad \text{for the Ladder level scheme} \tag{3.20a}$$

$$\phi_d = \frac{\pi}{2} - \phi_p + \phi_s \quad \text{for the } \Lambda \text{ level scheme} \tag{3.20b}$$

It is important to understand what ϕ_p, ϕ_s and ϕ_d are.

The Rabi frequency is defined as [21, 28]

$$\Omega(t) = -\frac{\mu_{ab}E_0(t)}{\hbar}. \tag{3.21}$$

where

$$\mu_{ab} = e\,\langle a|\,\hat{\boldsymbol{\varepsilon}}\cdot\mathbf{r}\,|b\rangle \tag{3.22}$$

is the transition dipole moment between states $|a\rangle$ and $|b\rangle$, $\hat{\boldsymbol{\varepsilon}}$ is the polarization of the light and $E_0(t)$ is the electric field amplitude of the electromagnetic wave

$$\mathbf{E}(\mathbf{r},t) = \hat{\boldsymbol{\varepsilon}}E_0(t)e^{\mathrm{i}(\mathbf{k}\cdot\mathbf{r}-\omega t)} + \hat{\boldsymbol{\varepsilon}}^* E_0^*(t)e^{-\mathrm{i}(\mathbf{k}\cdot\mathbf{r}-\omega t)}. \tag{3.23}$$

The appearance in Eqs. (3.16) of $\Omega_{p/s}^*(t)$ rather than $\Omega_{p/s}(t)$, or vice versa, follows the convention of pairing Ω with the positive-frequency amplitude E_0 and pairing Ω^* with E_0^*.

Notice that

$$E_0(t) = e^{\mathrm{i}\varphi} |E_0(t)| \tag{3.24}$$

where φ is the phase of the electromagnetic wave. So the phase of the Rabi frequency is

$$e^{\mathrm{i}\phi} = e^{\mathrm{i}\varphi} \frac{\langle a| \hat{\boldsymbol{\varepsilon}} \cdot \mathbf{r} |b\rangle}{|\langle a| \hat{\boldsymbol{\varepsilon}} \cdot \mathbf{r} |b\rangle|} \quad \Rightarrow \tag{3.25a}$$

$$\Rightarrow \quad \phi = \varphi - \mathrm{i} \ln \frac{\langle a| \hat{\boldsymbol{\varepsilon}} \cdot \mathbf{r} |b\rangle}{|\langle a| \hat{\boldsymbol{\varepsilon}} \cdot \mathbf{r} |b\rangle|} \tag{3.25b}$$

The last term in Eq. (3.25b) depends on the wavefunctions of the states $|a\rangle$ and $|b\rangle$ and on the direction of the dipole moment with respect to the light polarization.

In conclusion the phases of the matrix elements of the pump and Stokes pulses are defined by the basis set used to write the Hamiltonian matrix, the direction of the dipole moment with respect to the polarization of the light and the phases of the pump and Stokes electric fields. The physical meaning of the phase of the detuning pulse depends on the type of interaction with which it is actually applied to a system. Two type of interactions are discussed in Sec. 3.4 and Sec. 3.5.

3.3 Adiabatic and Super-Adiabatic Following

If we apply the total Hamiltonian $H(t) = H_0(t) + H_1(t)$ to the system starting in an adiabatic state of the Hamiltonian $H_0(t)$, then the exact solution of the Schrödinger equation

$$\mathrm{i}\hbar \frac{\partial}{\partial t} |\psi(t)\rangle = H(t) |\psi(t)\rangle \tag{3.26}$$

is that adiabatic state of $H_0(t)$. With the initial condition $|\psi(t_i)\rangle = |1\rangle = |a_0(t_i)\rangle$, for all the evolution process will be

$$|\langle a_0(t)|\psi(t)\rangle| = 1, \tag{3.27}$$

i.e., the adiabaticity (with respect to the Hamiltonian $H_0(t)$) is exactly 1.

This evolution is super-adiabatic for any values of parameters that characterize the slowness of the STIRAP. These parameters are the amplitude of the pump and Stokes Rabi frequency and the time of the process. A more general definition of typical STIRAP pulses of that given in Eq. (2.20) is

$$\begin{aligned} \Omega_p(t) &= A f(t,\tau) \\ \Omega_s(t) &= B g(t,\tau) \end{aligned} \tag{3.28}$$

where $f(t)$ and $g(t)$ are the pulse envelope of unit maximum value, A and B are the maximum Rabi Frequency for the pump and Stokes pulse and τ is a measure of the time of overlap of the pulses. As stated in Eq. (2.21), the condition for the adiabatic following in STIRAP is

$$A\tau > 20 \quad \text{and} \quad B\tau > 20. \tag{3.29}$$

In the case of super-adiabatic STIRAP the condition (3.29) is no longer required. As mentioned in the opening of the chapter, in the limiting case we can also take $A = B \to 0$ and $\tau \to 0^+$.

- $A = B \to 0$ means that the pump and Stokes pulse are turned off. In this case, however, the detuning pulse
$$\Omega_d(t) = 2\dot{\theta}(t) \tag{3.30}$$
is different from zero. In fact we can assume that, in the formula for $\theta(t)$, the two amplitude A and B simplify
$$\tan\theta(t) = \frac{\Omega_p(t)}{\Omega_s(t)} = \frac{Af(t,\tau)}{Bg(t,\tau)} = \frac{f(t,\tau)}{g(t,\tau)}. \tag{3.31}$$
Matrix elements $H_1(t)_{12}$ and $H_1(t)_{23}$ instead are zero. In fact they are proportional to $\dot{\phi}(t)$ (see Eqs. (3.6)), $\phi(t)$ defined in Eq. (2.8).

  Eq. (3.7b) demonstrate that $\Delta_p(t) = 0$ implies $\dot{\phi}(t) = 0$. But if $\Delta_p(t) \neq 0$, following Eq. (2.8) the condition $A = B \to 0$ implies $\phi(t) = 0$. Therefore $\dot{\phi}(t) = 0$ and then $H_1(t)_{12} = H_1(t)_{23} = 0$.

- $\tau \to 0^+$ means that the pulses are extremely rapid. The condition $\tau = 0$ cannot be applied because of the definition (2.2) of the counter-intuitive pulse sequence of the STIRAP: if $\tau = 0$ the two pulse are not ordered counter-intuitively.

  Remembering that the detuning pulse is a π-pulse, very small τ imply that the amplitude of the detuning pulse is very large. In fact the integral of the detuning pulse in an interval of time of the order of τ must be equal to π
$$A(t) = \int_{t_i}^{t_f} \Omega_d(t')dt' = \pi \tag{3.32}$$
with $t_f - t_i \approx \tau$. If $\tau \to 0^+$, then $\Omega_d(t) \to \infty$ for $t_i < t < t_f$.

In conclusion the system will follow an adiabatic state of the STIRAP Hamiltonian also if only the detuning pulse is applied
$$H(t) = \frac{\hbar}{2}\begin{pmatrix} 0 & 0 & \Omega_d(t) \\ 0 & 2\Delta_p(t) & 0 \\ \Omega_d^*(t) & 0 & 0 \end{pmatrix}. \tag{3.33}$$
For this reason we can say that the super-adiabatic STIRAP is a π-pulse. The evolution of the populations in states $|1\rangle$, $|2\rangle$ and $|3\rangle$ is completely defined by (the shape of) $\Omega_d(t)$, which is completely defined by (the shape of) $\Omega_p(t)$ and $\Omega_s(t)$.

3.4 Magnetic Dipole Transition

In a Λ system (see Fig. 3.2) the interaction between states $|1\rangle$ and $|3\rangle$ can take place with a magnetic dipole interaction via a low-frequency (i.e. non-radiative) magnetic field.

The Hamiltonian describing the interaction of an atom or molecule with an external static magnetic field is

$$H_B = \mu_B g_J \frac{\mathbf{J}\cdot\mathbf{B}}{\hbar} \tag{3.34}$$

with μ_B being the Bohr magneton, g_J the Landé factor, $\mathbf{J}$ the total atomic angular momentum and $\mathbf{B}$ the external magnetic field. The detuning pulse, then, must be

$$\Omega_d(t) = \mu_B \langle 1| g_J \frac{\mathbf{J}\cdot\mathbf{B}(t)}{\hbar} |3\rangle , \tag{3.35}$$

since μ_B and g_J are Real quantities, then

$$\phi_d = \frac{\langle 1|\, \mathbf{J}\cdot\mathbf{B}(t)\, |3\rangle}{|\langle 1|\, \mathbf{J}\cdot\mathbf{B}(t)\, |3\rangle|} \tag{3.36}$$

Eq. (3.36) means that the phase of the matrix element describing the detuning pulse is determined by the direction of the magnetic field with respect to the direction of the total angular momentum.

Ref. [26] proposed a simple example of population transfer between sub-levels of an atomic level having angular momentum $J = 1$. All of these three sub-levels have, for appropriate choice of polarization, potential electric dipole transition moments to a non-degenerate $J = 0$ level. By suitably choosing the polarization it is possible to create a Λ-linkage pattern involving only two low-energy states and the single intermediate excited state (see Fig. 3.4). We assume pump and Stokes pulses to have orthogonal linear polarizations. The arrangement is most clear if we use a Cartesian basis labeled by $|X\rangle$, $|Y\rangle$ and $|Z\rangle$ rather than the spherical basis of eigenstates of J_z, which bear labels of the magnetic quantum number $M_J = -1, 0, +1$. The connections between the two bases are

$$|\pm 1\rangle = \mp \frac{1}{\sqrt{2}} \left(|X\rangle \pm \mathrm{i}\, |Y\rangle\right), \quad |0\rangle = |Z\rangle \tag{3.37a}$$

and

$$\begin{aligned} |X\rangle &= \frac{1}{\sqrt{2}} \left(|-1\rangle - |+1\rangle\right), \quad |Z\rangle = |0\rangle . \\ |Y\rangle &= \frac{\mathrm{i}}{\sqrt{2}} \left(|-1\rangle + |+1\rangle\right), \end{aligned} \tag{3.37b}$$

In this case the condition (3.20b) is fulfilled because the matrix element $H(t)_{12}$ and $H(t)_{23}$ are Real while $H(t)_{13}$ is imaginary. In fact, with reference to Fig. 3.4, the magnetic field along the x axis gives

$$\langle Y|\, H_{13}\, |Z\rangle = \frac{\mu_B g_J}{\hbar} \langle Y|\, \mathbf{J}\cdot\mathbf{B}\, |Z\rangle = \frac{\mu_B g_J}{\hbar} B_x \langle Y|\, J_x\, |Z\rangle = -\mathrm{i}\frac{\mu_B g_J}{\hbar} B_x \tag{3.38}$$

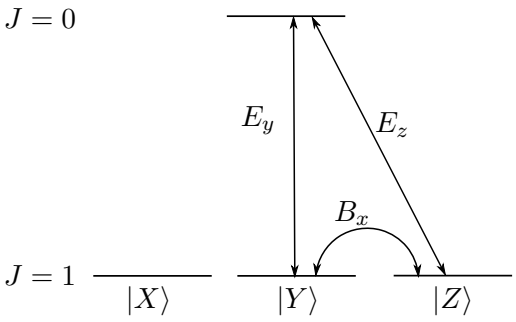

Figure 3.4: Configuration for Super-adiabatic STIRAP in a Λ system with magnetic sub-levels, defined in a Cartesian basis set linked to the eigenstates of J_i, $(i = x, y, z)$ as in Eqs. (3.37). The polarization of the pump and Stokes fields are linear and orthogonal to each other. If they have polarization along the y and z axis, then the detuning magnetic field must be aligned along the x axis.

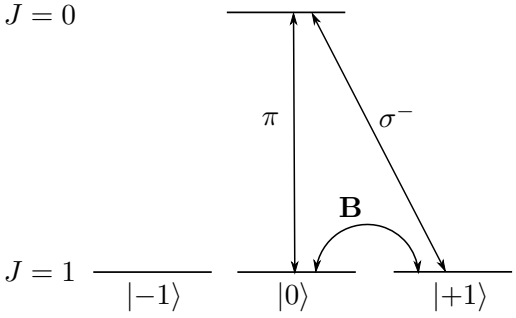

Figure 3.5: Configuration for Super-adiabatic STIRAP in a Λ system with magnetic sub-levels in the spherical basis set composed by eigenstates of J_z. The polarization of one of the lasers is π while the other is circular.

An other simple example which use the spherical basis is that represented in Fig. 3.5. In this case one of the pump or Stokes fields have π polarization and the other one have σ^- polarization. Assume that the quantization axis is the z axis and that the pump pulse have σ^- polarization and the Stokes pulse have π polarization. Then the wave vector of the pump pulse is along the z axis, while the Stokes pulse is linearly polarized along the z axis and its the wave vector is perpendicular to the z axis.

In this case the requirement of Eq. (3.20b) became

$$\phi_d = \frac{\pi}{2} - \varphi_p + \varphi_s \tag{3.39}$$

where φ_p and φ_s are the phase of the pump and Stokes electric fields. The phase ϕ_d fixed by Eq. (3.39) determines the orientation of the σ^+ circularly polarized magnetic field $\mathbf{B}$ in the $x - y$ plane. This configuration is very difficult to achieve in experimental setups because require the exact knowledge of the relative phase $(\varphi_p - \varphi_s)$ of the pump and Stokes electric field.

3.5 Two-photon Transition

In a ladder level scheme the interaction between states $|1\rangle$ and $|3\rangle$ can take place via two-photon transition (see Fig. 3.6).

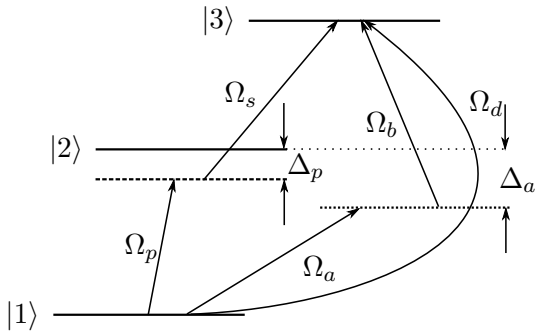

Figure 3.6: Ladder system with the detuning pulse achieved by two-photon transition.

If two new laser with Rabi frequencies $\Omega_a(t)$ and $\Omega_b(t)$ are added to the system, the two-photon resonance for these two lasers is fulfilled with the system far off one-photon resonance by the quantity Δ_a, the $\Omega_d(t)$ detuning is given by the two-photon Rabi frequency.

In a three-level system interacting in the usually way

$$1 \xrightarrow{\Omega_a} 2,\ 2 \xrightarrow{\Omega_b} 3 \tag{3.40}$$

with two lasers in two-photon resonance, the intermediate state $|2\rangle$ can be eliminated if it there is a "large" one-photon detuning [29].

The Hamiltonian is

$$H_{tp} = \frac{\hbar}{2} \begin{pmatrix} 0 & \Omega_a^* & 0 \\ \Omega_a & 2\Delta_a & \Omega_b^* \\ 0 & \Omega_b & 0 \end{pmatrix} \tag{3.41}$$

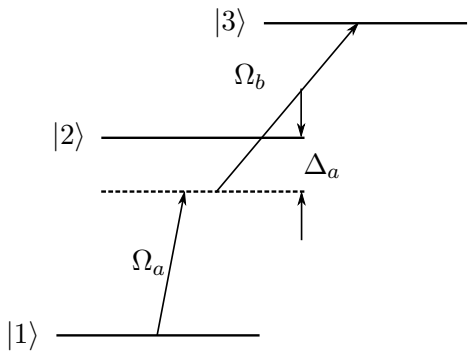

Figure 3.7: Ladder system with two-photon transition.

or equivalently (choosing differently the phases of the basis set)

$$H' = \frac{\hbar}{2}\begin{pmatrix} 0 & \Omega_a^* e^{-\imath\Delta_a t} & 0 \\ \Omega_a e^{\imath\Delta_a t} & 0 & \Omega_b^* e^{\imath\Delta_a t} \\ 0 & \Omega_b e^{-\imath\Delta_a t} & 0 \end{pmatrix} \tag{3.42}$$

Large detuning means

$$|\Delta_a| \gg |\Omega_a|, |\Omega_b| \tag{3.43}$$

In this case the system is equivalent to a two-level system with the effective Hamiltonian

$$H_{eff} = -\frac{\hbar}{4\Delta_a}\begin{pmatrix} |\Omega_a|^2 & \Omega_a^*\Omega_b^* \\ \Omega_a\Omega_b & |\Omega_b|^2 \end{pmatrix}. \tag{3.44}$$

The effective interaction then is

$$\Omega_R = -\frac{\Omega_a^*\Omega_b^*}{2\Delta_a}. \tag{3.45}$$

To achieve the super-adiabatic STIRAP we need to impose that the detuning pulse $\Omega_d(t)$ is equal to the effective interaction of two-photon transition Ω_R

$$\Omega_d(t) = \Omega_R(t) = -\frac{\Omega_a^*(t)\Omega_b^*(t)}{2\Delta_a(t)}. \tag{3.46}$$

A simple choice is $\Omega_a(t) = e^{\mathrm{i}\pi}\Omega_b(t) = -\Omega_b(t)$

$$\Omega_a(t) = \sqrt{2\Delta_a(t)\Omega_d^*(t)} \tag{3.47a}$$

$$\Omega_b(t) = -\sqrt{2\Delta_a(t)\Omega_d^*(t)} \tag{3.47b}$$

In addition to the pump and Stokes laser, the detuning pulse is achieved by two other laser in two photon resonance. The shape of these lasers must satisfy Eq. (3.46), so it depends on the shape of the pump and Stokes laser.

Even in this case the phases of the lasers is a critical point for actual experiment. In fact it is required the knowledge of the phase of the pump and Stokes laser and the control on the phase of the two new added lasers.

CHAPTER 4

Comparing Shapes

In this chapter we compare various dependence on time of STIRAP pulses. The condition for adiabatic following is (see Eq. (2.16)

$$\left|\frac{\dot{\Omega}_p(t)\Omega_s(t) - \Omega_p(t)\dot{\Omega}_s(t)}{\Omega_p(t)^2 + \Omega_s(t)^2}\right| = \left|\dot{\theta}(t)\right| = \left|\frac{\Omega_d(t)}{2}\right| \ll \frac{|\lambda_\pm(t) - \lambda_0(t)|}{\hbar} \tag{4.1}$$

So we define the *adiabaticity parameter*

$$\epsilon(t) = \frac{\hbar}{2}\left|\frac{\Omega_d(t)}{\lambda_\pm(t) - \lambda_0(t)}\right| \tag{4.2}$$

and the condition for adiabatic following is $\epsilon(t) \ll 1$. The inequality (4.2) must hold for all the time of the process.

For each kind of pulses we calculate the detuning pulse (3.10) and $\Omega_0(t)$ (2.4) and we plot:

- the maximum of $\epsilon(t)$ as a function of the parameters of the pulses,
- the final fidelity as a function of the parameters of the pulses,

Then we choose two values of the Rabi frequencies and we plot:

- the pump, Stokes and detuning pulse,
- the adiabaticity parameter $\epsilon(t)$,
- the evolution of the population for the two values of the Rabi frequencies,
- the adiabaticity of the evolution $|\langle 3|\psi(t)\rangle|$,
- the Super-Adiabatic evolution.

All graphs have been obtained by solving numerically the Schrödinger equation.

All plots are done in arbitrary time units.

4.1 Exponential Pulses

Consider exponential pulses [30]

$$\begin{aligned} \Omega_p(t) &= \frac{A}{\sqrt{1+e^{-t/\tau}}} \\ \Omega_s(t) &= \frac{A}{\sqrt{1+e^{+t/\tau}}} \end{aligned} \tag{4.3}$$

Detuning pulse and $\Omega_0(t)$

$$\begin{aligned} \Omega_0^2(t) &= A^2 \\ \Omega_d(t) &= \frac{1}{\tau}\frac{1}{\sqrt{2+e^{-t/\tau}+e^{t/\tau}}} = \frac{1}{2\tau\cosh\left(\frac{t}{2\tau}\right)} \end{aligned} \tag{4.4}$$

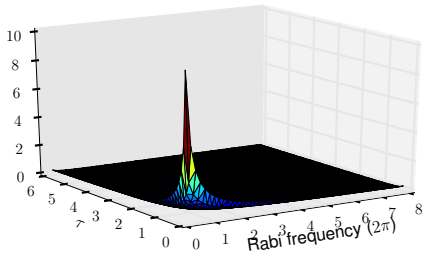

(a) Maximum of ϵ as a function of A and τ.

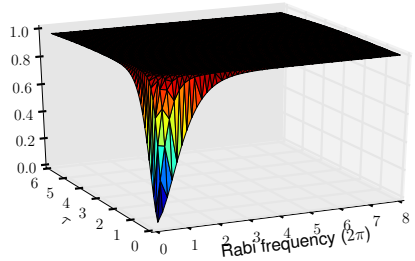

(b) Final fidelity as a function of A and τ.

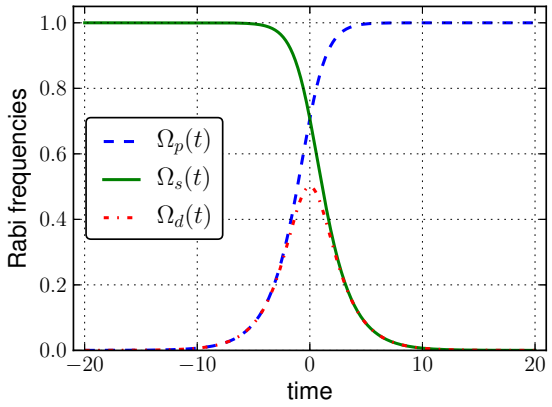

(c) Exponential pulses and Ω_d.

We look at the evolution for $\tau = 1$, $A = 1$ and for $\tau = 1$, $A = 2$.

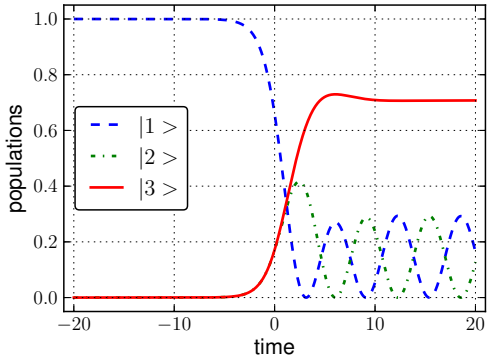

(d) Populations with $A = 1$ and $\tau = 1$.

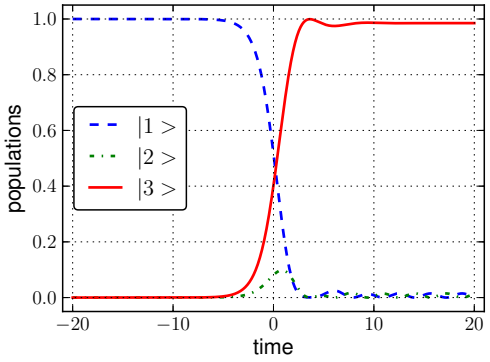

(e) Populations with $A = 2$ and $\tau = 1$.

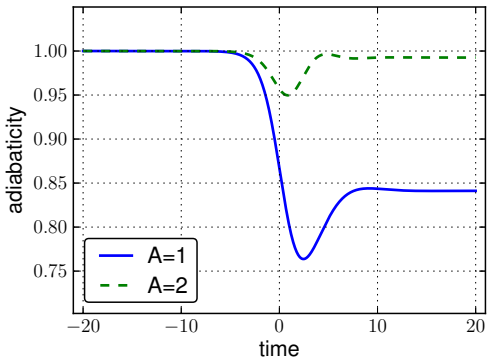

(f) Adiabaticity with $A = 1, 2$ and $\tau = 1$.

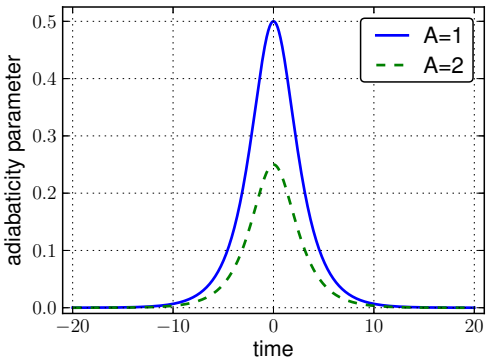

(g) $\epsilon(t)$ with $A = 1, 2$ and $\tau = 1$.

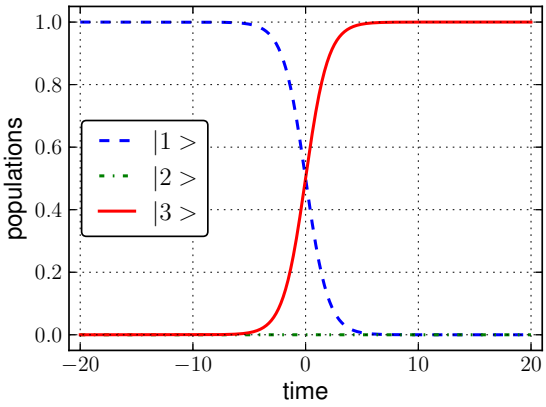

(h) Super-Adiabatic evolution.

Figure 4.1: Plots for exponential pulses.

4.2 Secant Pulses

Consider pulses of the type [30]:

$$\begin{aligned}\Omega_p(t) &= A\,\mathrm{sech}\,\frac{t-\tau}{T}\\ \Omega_s(t) &= A\,\mathrm{sech}\,\frac{t+\tau}{T}.\end{aligned} \tag{4.5}$$

We impose $T = 2\tau$. In this case the detuning pulse and $\Omega_0(t)$ are

$$\begin{aligned}\Omega_0^2(t) &= A^2\left[\mathrm{sech}^2\left(\frac{t-\tau}{T}\right)+\mathrm{sech}^2\left(\frac{t+\tau}{T}\right)\right]\\ \Omega_d(t) &= \frac{2\sinh\left(\frac{2\tau}{T}\right)}{T\left[1+\cosh\left(\frac{2t}{T}\right)\cosh\left(\frac{2\tau}{T}\right)\right]}\end{aligned} \tag{4.6}$$

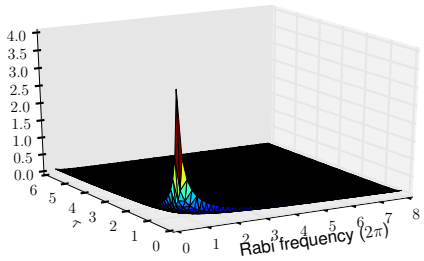

(a) Maximum of ϵ as a function of A and τ.

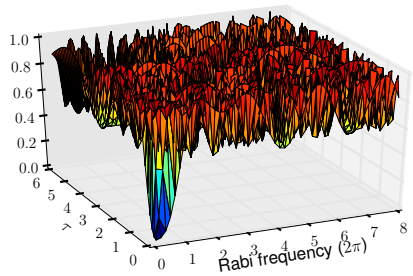

(b) Final fidelity as a function of A and τ.

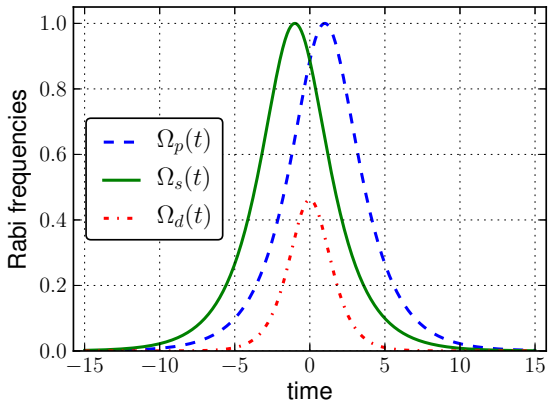

(c) Sech pulses and Ω_d with $\tau = 1$.

We look at the evolution for $\tau = 1$, $A = 1$ and for $\tau = 1$, $A = 2$.

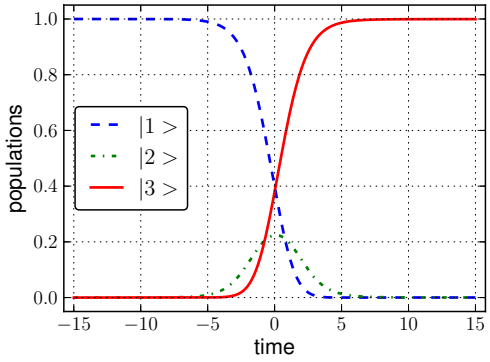

(d) Populations with $A = 1$ and $\tau = 1$.

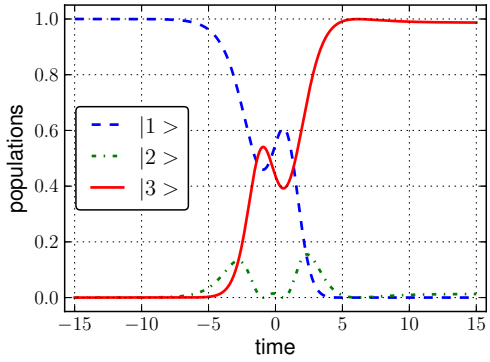

(e) Populations with $A = 2$ and $\tau = 1$.

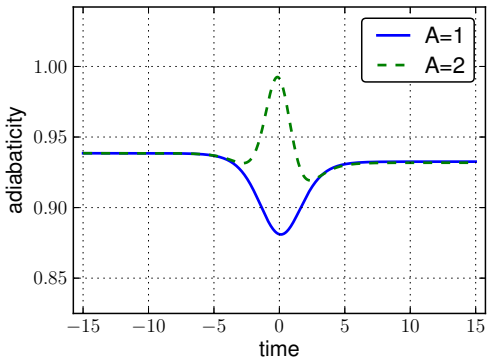

(f) Adiabaticity with $A = 1, 2$ and $\tau = 1$.

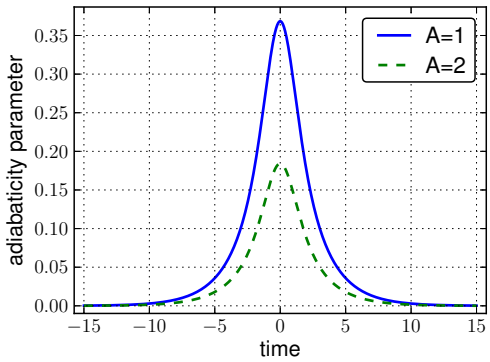

(g) $\epsilon(t)$ with $A = 10, 20$ and $\tau = 1$.

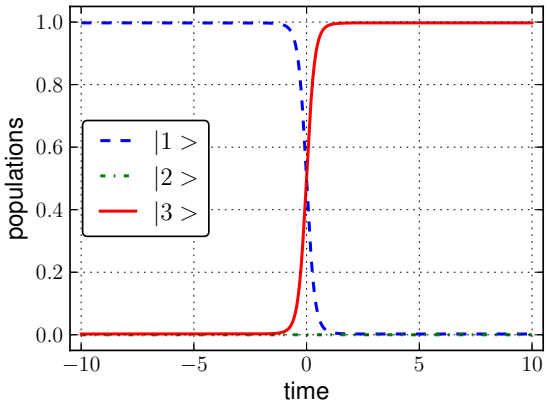

(h) Super-Adiabatic evolution.

Figure 4.2: Plots for secant pulses.

4.3 Gaussian Pulses

Consider pulses of the type [30]:

$$\begin{aligned}\Omega_p(t) &= Ae^{-\left(\frac{t-\tau}{T}\right)^2} \\ \Omega_s(t) &= Ae^{-\left(\frac{t+\tau}{T}\right)^2}\end{aligned} \tag{4.7}$$

with $T = 3\tau$. In this case:

$$\begin{aligned}\Omega_0^2(t) &= 2A^2 e^{-\frac{2\left(t^2+\tau^2\right)}{T^2}} \cosh\left(\frac{4t\tau}{T^2}\right) \\ \Omega_d(t) &= \frac{4\tau}{T^2 \cosh\left(\frac{4t\tau}{T^2}\right)}\end{aligned} \tag{4.8}$$

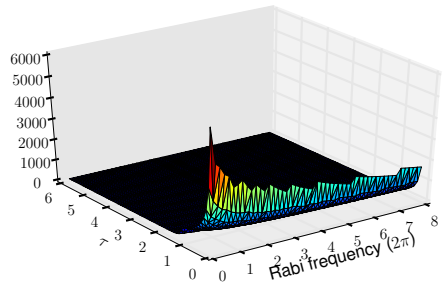

(a) Maximum of ϵ as a function of A and τ.

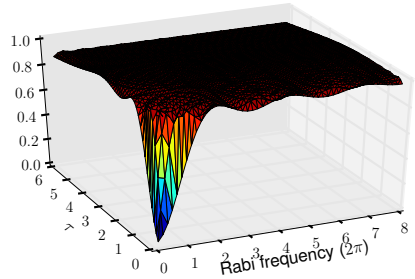

(b) Final fidelity as a function of A and τ.

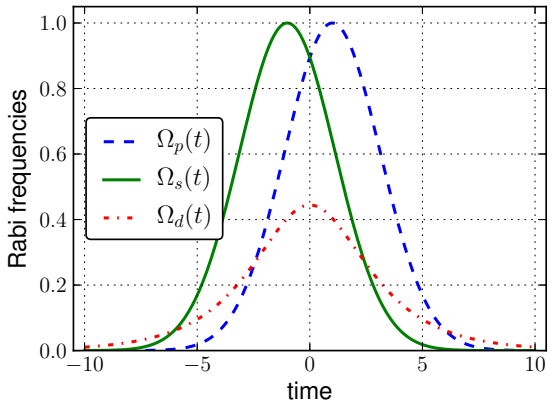

(c) Gaussian pulses and Ω_d with $\tau = 1$.

We look at the evolution for $\tau = 1$, $A = 1$ and for $\tau = 1$, $A = 2$.

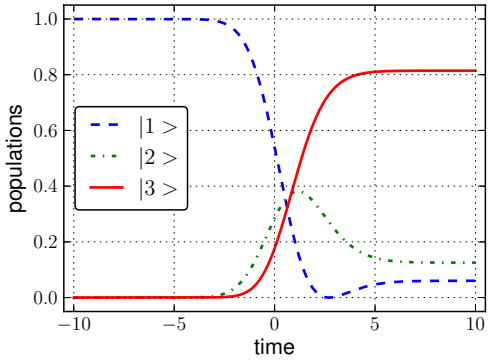

(d) Populations with $A = 1$ and $\tau = 1$.

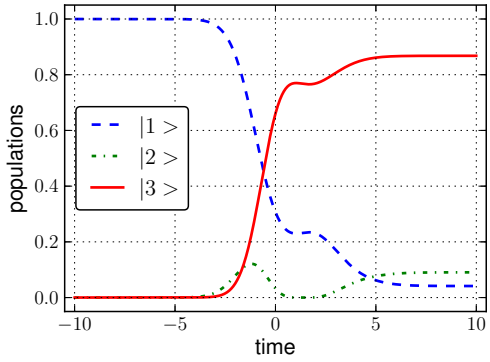

(e) Populations with $A = 2$ and $\tau = 1$.

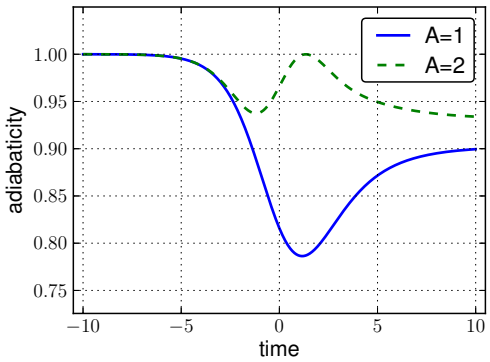

(f) Adiabaticity with $A = 1, 2$ and $\tau = 1$.

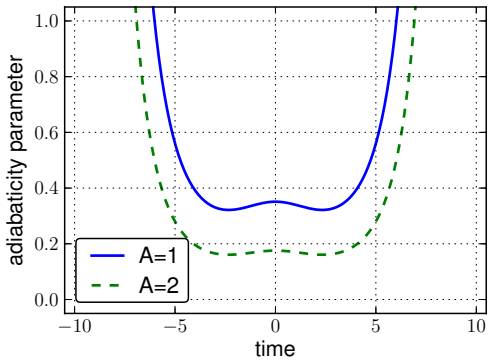

(g) $\epsilon(t)$ with $A = 1, 2$ and $\tau = 1$.

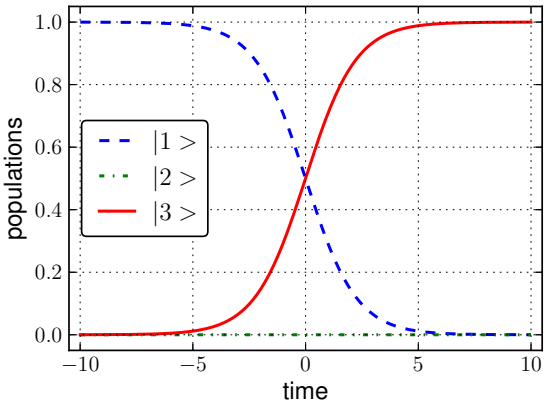

(h) Super-Adiabatic evolution.

Figure 4.3: Plots for Gaussian pulses.

4.4 $\sin^4$ Pulses

Consider pulses of the type [23]

$$\begin{aligned}\Omega_p(t) &= \begin{cases} A\sin^4\frac{\pi(t-\tau)}{T} & \tau < t < \tau + T \\ 0 & \text{otherwise} \end{cases} \\ \Omega_s(t) &= \begin{cases} A\sin^4\frac{\pi t}{T} & 0 < t < T \\ 0 & \text{otherwise} \end{cases}\end{aligned} \tag{4.9}$$

And then the detuning pulse and $\Omega(0)$

$$\begin{aligned}\Omega_0^2(t) &= A^2\left[\sin^8\left(\frac{\pi}{T}(t-\tau)\right)\right] + \sin^8\left(\frac{\pi}{T}t\right) \quad \text{for} \quad \tau < t < T \\ \Omega_d(t) &= \frac{8\sin\left(\frac{\pi\tau}{T}\right)\sin^3\left(\frac{\pi}{T}(t-\tau)\right)\sin^3\left(\frac{\pi}{T}\tau\right)}{\sin^8\left(\frac{\pi}{T}(t-\tau)\right) + \sin^8\left(\frac{\pi}{T}t\right)} \quad \text{for} \quad \tau < t < T\end{aligned} \tag{4.10}$$

T has been chosen to be $T = 5\tau$.

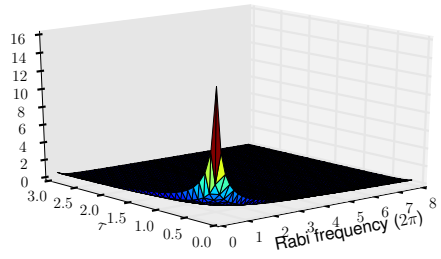

(a) Maximum of ϵ as a function of A and τ.

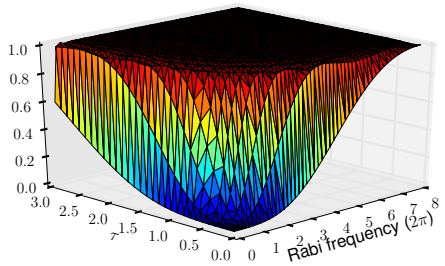

(b) Final fidelity as a function of A and τ.

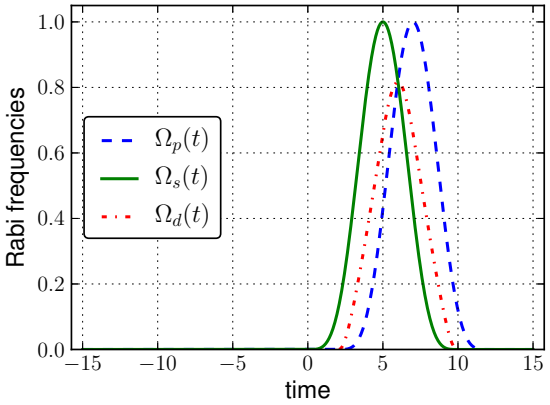

(c) $\sin^4$ pulses and Ω_d with $\tau = 1$.

We look at the evolution for $\tau = 2$, $A = 1$ and for $\tau = 2$, $A = 2$.

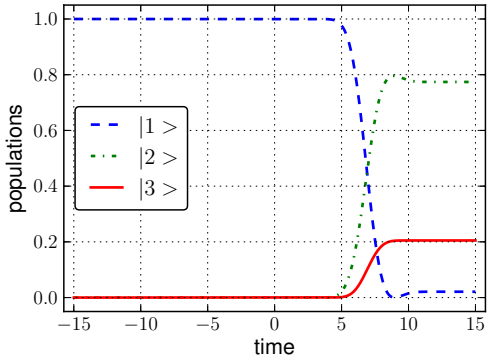

(d) Populations with $A = 1$ and $\tau = 2$.

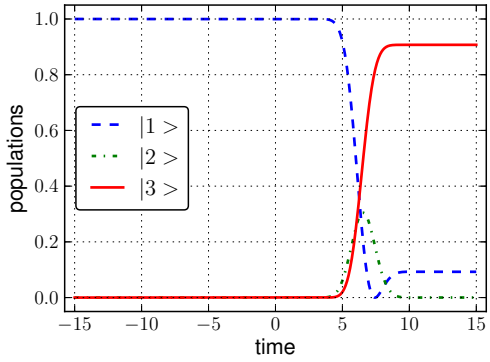

(e) Populations with $A = 2$ and $\tau = 2$.

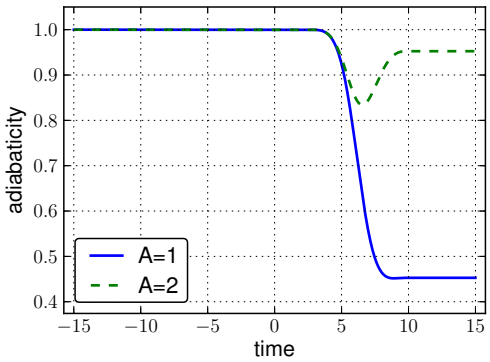

(f) Adiabaticity with $A = 1, 2$ and $\tau = 2$.

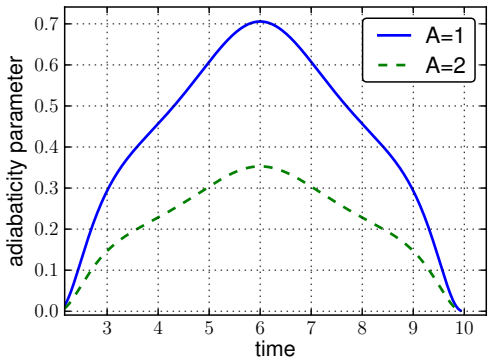

(g) $\epsilon(t)$ with $A = 1, 2$ and $\tau = 2$.

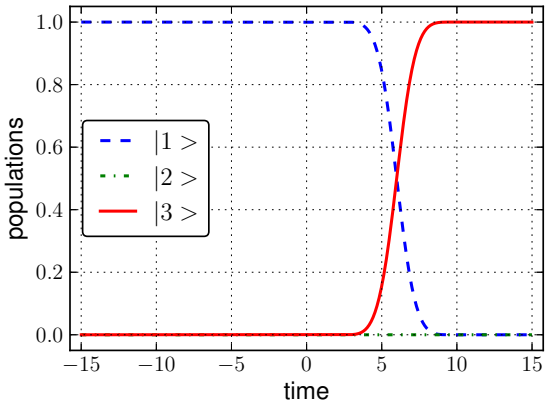

(h) Super-Adiabatic evolution.

Figure 4.4: Plots for $\sin^4$ pulses.

4.5 Carroll Hioe type 1 Pulses

Consider pulses of the type [31]:

$$\begin{aligned}\Omega_p(t) &= \frac{A}{\tau}\operatorname{sech}\frac{t}{\tau}\\ \Omega_s(t) &= \frac{\alpha A}{\tau}\sqrt{2\left(1-\tanh\frac{t}{\tau}\right)}\end{aligned} \tag{4.11}$$

with $\alpha = 0.3$. In This case:

$$\begin{aligned}\Omega_0^2(t) &= \frac{A^2\left[\operatorname{sech}^2\frac{t}{\tau}+2\alpha^2\left(1-\tanh\frac{t}{\tau}\right)\right]}{\tau^2}\\ \Omega_d(t) &= \frac{2\alpha e^{\frac{t}{\tau}}}{\tau\left(\alpha^2+e^{\frac{2t}{\tau}}\left(1+\alpha^2\right)\right)\sqrt{1+e^{\frac{2t}{\tau}}}}\end{aligned} \tag{4.12}$$

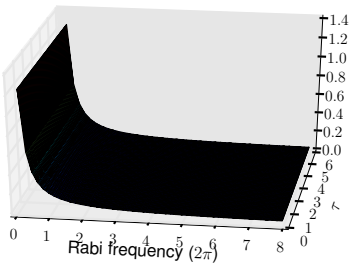

(a) Maximum of ϵ as a function of A and τ.

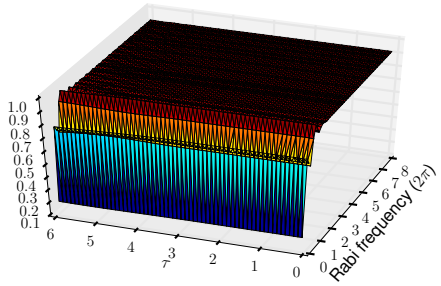

(b) Final fidelity as a function of A and τ.

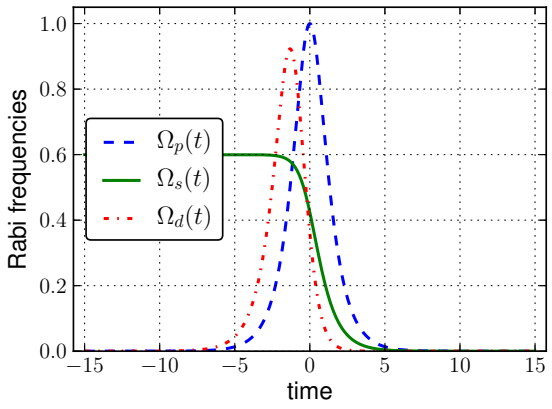

(c) C.H.1 pulses and Ω_d.

We look at the evolution for $\tau = 1$, $A = 1$ and for $\tau = 1$, $A = 2$.

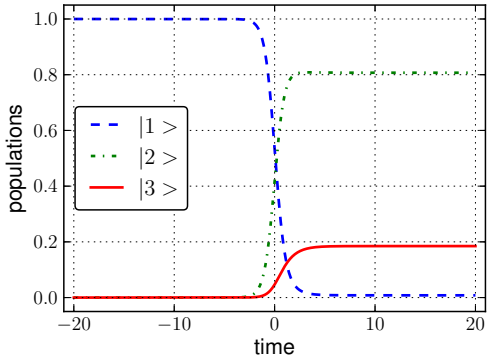

(d) Populations with $A = 1$ and $\tau = 1$.

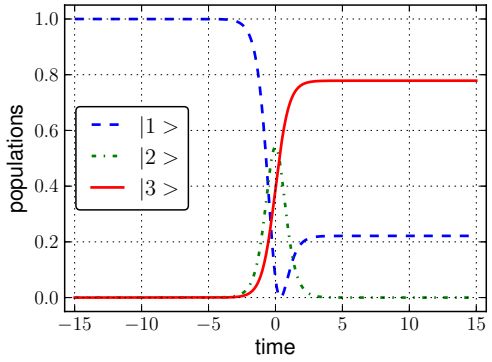

(e) Populations with $A = 2$ and $\tau = 1$.

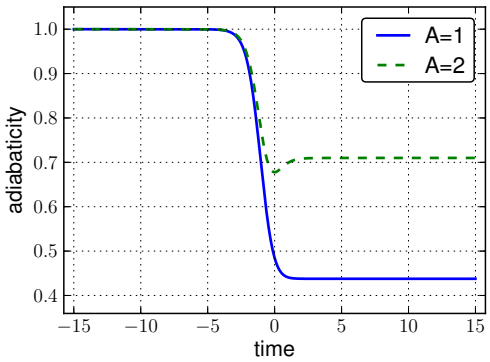

(f) Adiabaticity with $A = 1, 2$ and $\tau = 1$.

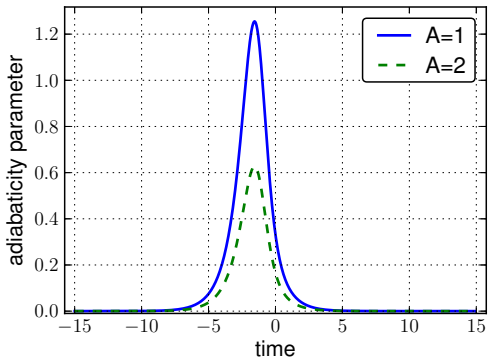

(g) $\epsilon(t)$ with $A = 1, 2$ and $\tau = 1$.

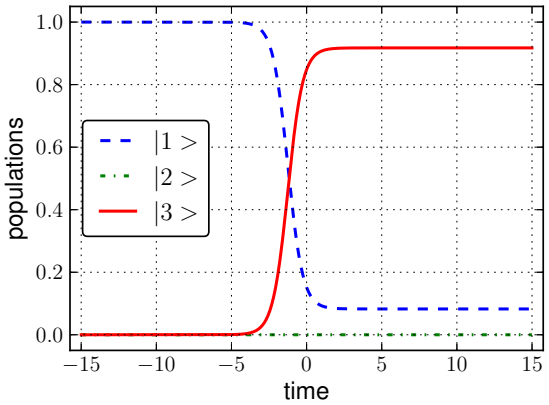

(h) Super-Adiabatic evolution.

Figure 4.5: Plots for C.H.1 pulses.

4.6 Carroll Hioe type 2 Pulses

Let us consider pulses of the type [31]:

$$\begin{aligned}\Omega_p(t) &= \frac{A}{\tau}\sqrt{\frac{1}{2}\left(1-\tanh\frac{t}{\tau}\right)}\,\operatorname{sech}\frac{t}{\tau}\\ \Omega_s(t) &= \frac{\alpha A}{\tau}\left(1-\tanh\frac{t}{\tau}\right)\end{aligned} \tag{4.13}$$

with $\alpha = 0.3$. In This case:

$$\begin{aligned}\Omega_0^2(t) &= \frac{A^2\alpha\sqrt{\frac{1}{2}\left(1-\tanh\left(\frac{t}{\tau}\right)\right)}}{2\tau\left[\left(\frac{1}{2}+\alpha^2\right)\cosh\left(\frac{t}{\tau}\right)+\frac{1}{2}\sinh\left(\frac{t}{\tau}\right)\right]}\\ \Omega_d(t) &= \frac{2\left(1-\tanh\frac{t}{\tau}\right)\left[\frac{1}{2}\operatorname{sech}^2\frac{t}{\tau}+\alpha^2\left(1-\tanh\frac{t}{\tau}\right)\right]}{\tau^2}\end{aligned} \tag{4.14}$$

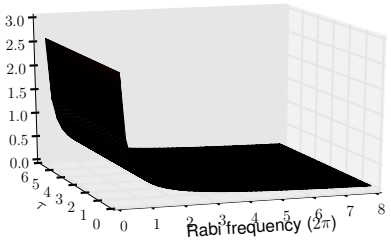

(a) Maximum of ϵ as a function of A and τ.

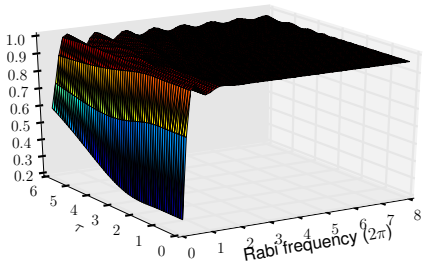

(b) Final fidelity as a function of A and τ.

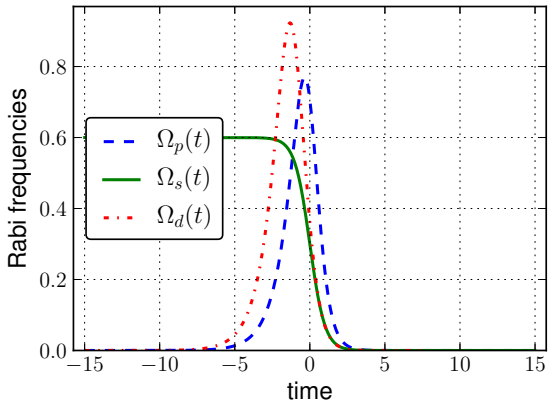

(c) C.H.1 pulses and Ω_d.

We look at the evolution for $\tau = 1$, $A = 2$ and for $\tau = 1$, $A = 5$.

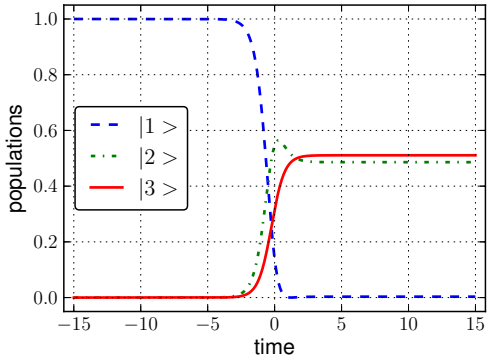

(d) Populations with $A = 2$ and $\tau = 1$.

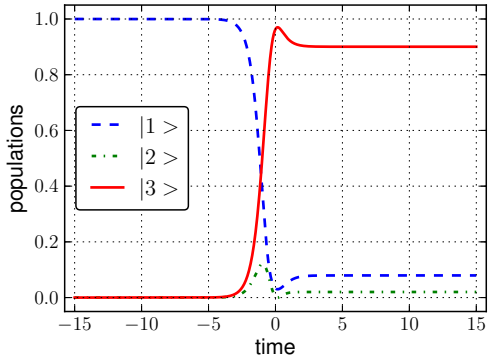

(e) Populations with $A = 5$ and $\tau = 1$.

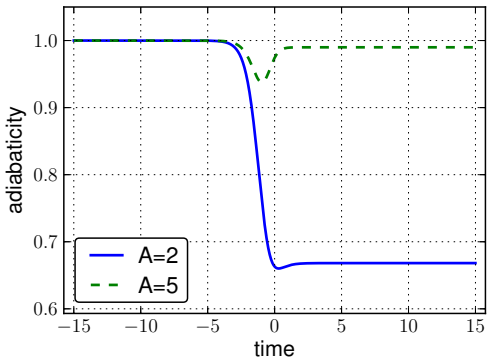

(f) Adiabaticity with $A = 2, 5$ and $\tau = 1$.

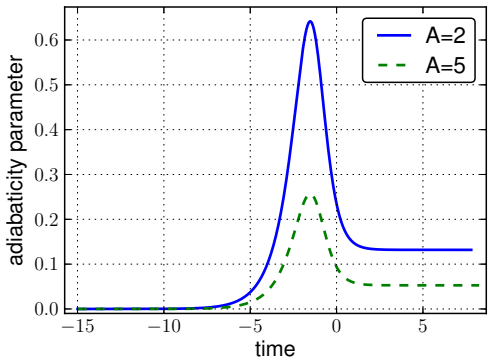

(g) $\epsilon(t)$ with $A = 2, 5$ and $\tau = 1$.

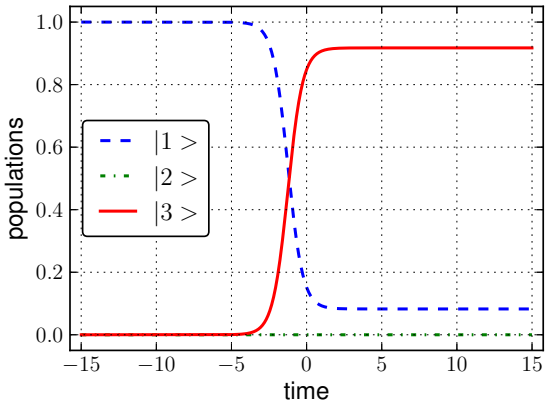

(h) Super-Adiabatic evolution.

Figure 4.6: Plots for C.H.1 pulses.

4.7 Sinusoidal Pulses

Consider pulses of the type

$$\Omega_p(t) = \begin{cases} 0 & t < 0 \\ A \sin\left(\frac{\pi t}{2\tau}\right) & 0 < t < \tau \\ A & \tau < t \end{cases}$$
$$\Omega_s(t) = \begin{cases} A & t < 0 \\ A \cos\left(\frac{\pi t}{2\tau}\right) & 0 < t < \tau \\ 0 & \tau < t \end{cases} \tag{4.15}$$

In this case

$$\Omega_0(t) = A^2 \tag{4.16}$$

$$\Omega_d(t) = \begin{cases} \frac{\pi}{\tau} & 0 < t < \tau \\ 0 & t < 0,\ \tau < t \end{cases} \tag{4.17}$$

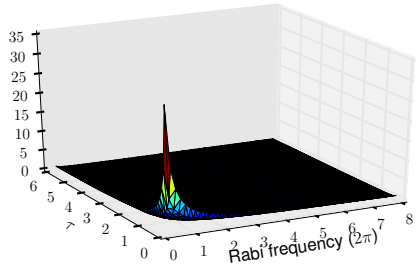

(a) Maximum of ϵ as a function of A and τ.

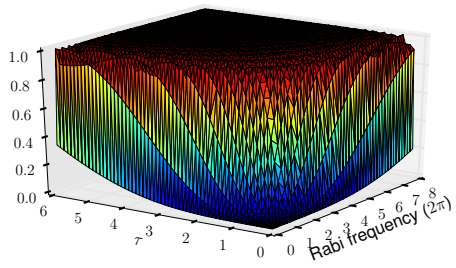

(b) Final fidelity as a function of A and τ.

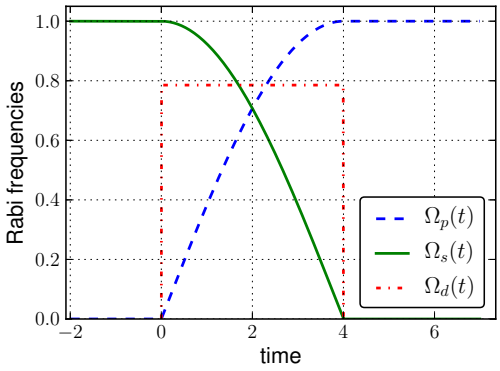

(c) C.H.1 pulses and Ω_d.

We look at the evolution for $\tau = 4$, $A = 2$ and for $\tau = 4$, $A = 5$.

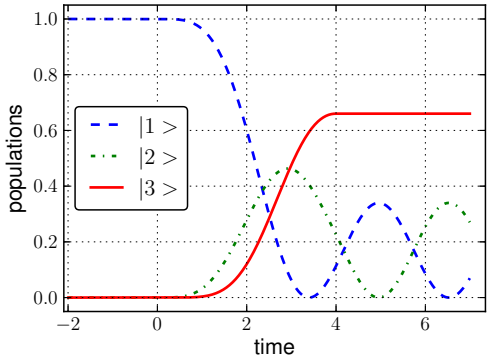

(d) Populations with $A = 2$ and $\tau = 4$.

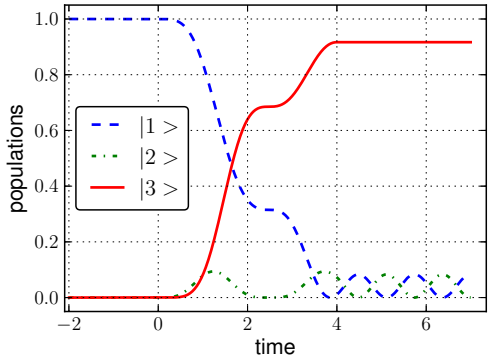

(e) Populations with $A = 5$ and $\tau = 4$.

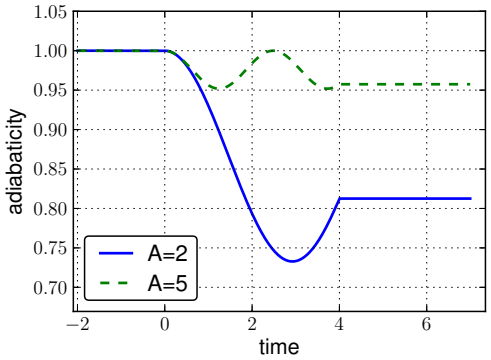

(f) Adiabaticity with $A = 2, 5$ and $\tau = 4$.

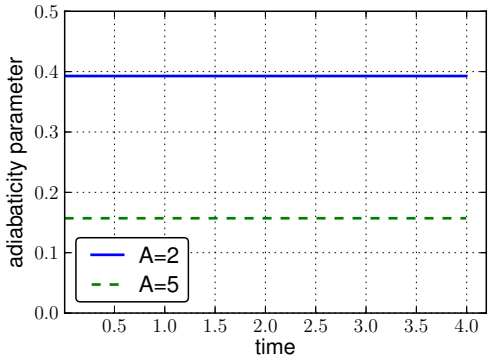

(g) $\epsilon(t)$ with $A = 2, 5$ and $\tau = 4$.

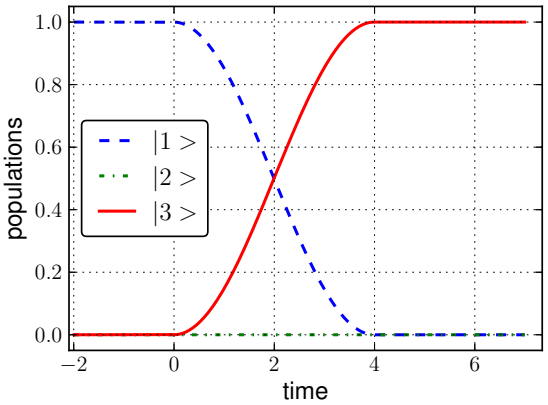

(h) Super-Adiabatic evolution.

Figure 4.7: Plots for Sinusoidal pulses.

4.8 Conclusion

In this paragraph we compare five of the seven kind of STIRAP pulses described above. In particular we study the time needed to achieve 0.90 fidelity. We do not compare Carroll and Hioe type pulses because they are not intended to reach so high fidelity, their final fidelity depends on the parameter α and we will not to study it here.

In Figs. 4.8 and 4.9 the time of the process is plotted. The results have been obtained by numerical simulations. The time of the process is defined as in the following:

$$|\psi(t_1)\rangle = a_1 |1\rangle + a_2 |2\rangle + a_3 |3\rangle , \text{ and } |a_1|^2 = 0.99 \tag{4.18a}$$

$$|\psi(t_2)\rangle = a_1 |1\rangle + a_2 |2\rangle + a_3 |3\rangle , \text{ and } |a_3|^2 = 0.9 \tag{4.18b}$$

$$T_{TOT} = t_2 - t_1, \tag{4.18c}$$

i.e. the time of the process T_{TOT} is the time necessary to transfer 90% of the population to the final state starting with 99% of population in the initial state.

For comparison the quantum speed limit has been plotted together with the STIRAP pulses. The quantum speed limit is defined

$$t = \frac{\pi}{A}. \tag{4.19}$$

As expected, the transfer cannot be faster then the quantum speed limit.

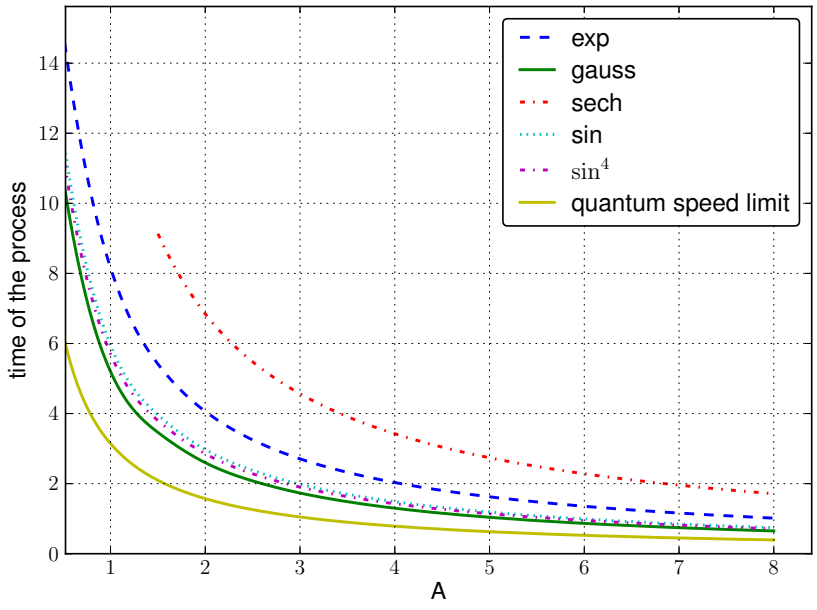

Figure 4.8: Time of the process for various pulses.

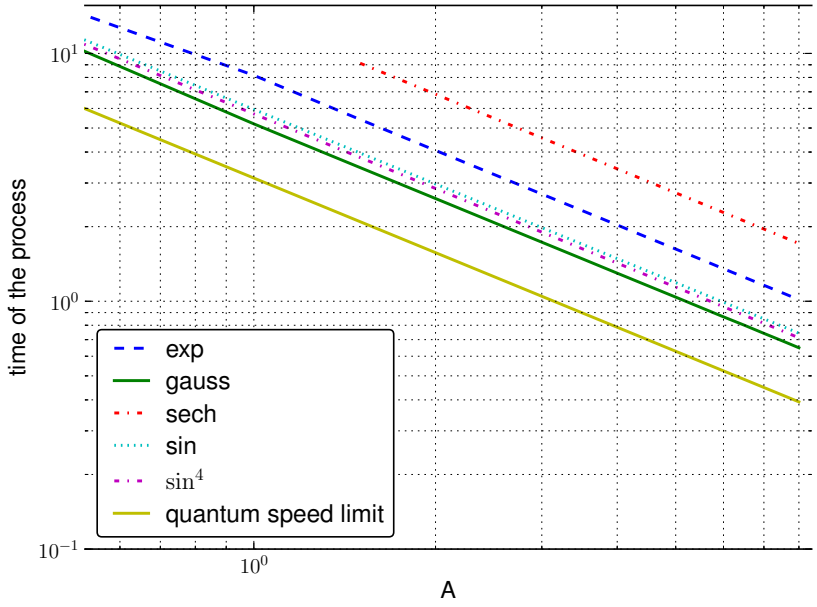

Figure 4.9: Time of the process for various pulses in log scale.

We see in Figs. 4.8 and 4.9 that there is difference in the time needed to achieve high fidelity between different STIRAP pulses. With this study we can say that the faster one is the STIRAP with Gaussian pulses. However in this work a systematic study of optimization for the transfer velocity has not been done and this result can be seen as indicative, and it is not clear if some special pulse shape could improve the transfer velocity. Notice that such question was not examined in the two-level case of Bason et al. [13].

CHAPTER 5

Robustness

In this chapter we study the robustness of the STIRAP process and of its super-adiabatic expansion. The robustness is a way to understand how non-ideal experimental condition can affect the fidelity of the transfer.

Two important quantities to evaluate the transfer process are the fidelity, i.e., the population in final target state $|3\rangle$ at the end of the process, defined as

$$F = |\langle 3|\psi(+\infty)\rangle|^2 \tag{5.1}$$

and the population loss in the intermediate state $|2\rangle$ during the evolution. For systems without relaxation there is not population loss, so another quantity that can be used to study the robustness is the maximum of population found in the intermediate state during the evolution

$$m = \max_{\forall t} |\langle 2|\psi(t)\rangle|^2. \tag{5.2}$$

5.1 STIRAP

Consider Gaussian pulses for the pump and Stokes laser of the type

$$\begin{aligned} \Omega_p(t) &= Ae^{-\left(\frac{t-\tau}{T}\right)^2} \\ \Omega_s(t) &= Ae^{-\left(\frac{t+\tau}{T}\right)^2} \end{aligned} \tag{5.3}$$

The integral over time of these Rabi frequencies (5.3) are

$$\int_{-\infty}^{+\infty} \Omega_{p/s}(t)dt = AT\sqrt{\pi} \tag{5.4}$$

We have four time parameters describing the lasers and the atom:

- A is the maximum Rabi frequency,

- T describe the duration of each pulse,
- 2τ is the delay between them and we can consider it as a measure of their overlap,
- Γ is the decay rate of the intermediate state.

There is a kind of invariance of time scale. In fact defined three constants c_1, c_2 and c_3, the evolution is the same one (except for a time scale factor) for any A, T, τ and Γ that satisfy

$$\begin{cases} AT = c_1 \\ A\tau = c_2 \\ \Gamma T = c_3 \end{cases} . \tag{5.5}$$

Therefore the free parameters determining the final fidelity and losses are only three, i.e. $F = F(c_1, c_2, c_3)$ and the same for the losses.

We set a temporal scale by fixing $T = 1.5\,\mu$s. We study with numerical simulations the evolution process as a function of A and τ, for three cases: $\Gamma \ll T^{-1}$, $\Gamma \approx T^{-1}$ and $\Gamma \gg T^{-1}$.

Notice that negative τ means that the pulse sequence is not counter-intuitive: first arrive the pump pulse and after a time -2τ arrive the Stokes pulse. So the process for negative valued τ is not the STIRAP evolution.

5.1.1 STIRAP without relaxation

Consider the case in which there is no relaxation of the states, i.e. all the three states have infinite life-time. This is the case $\Gamma = 0$. In such a situation there is not population loss in the intermediate state. The results of the numerical simulations are plotted in Fig. 5.1: (a) represents the fidelity F of the process and (b) the maximum m of population of the intermediate state.

In Fig. 5.1a it can be noticed, as expected, the Rabi oscillations, that appears for $\tau \lesssim 0.4\,\mu$s. For small Rabi frequency, large delay and counter-intuitive pulse sequence, i.e. the upper left part of the plot, the Rabi oscillations vanish. This happen because the two pulses are too delayed and their overlap is small.

The region $\tau > 0$ represent the STIRAP with counter-intuitive pulse sequence. In this region there is a wide range of values that allow complete transfer of population. For larger values of Rabi frequency there is a larger interval of delays that allow the transfer of almost all population to the final state.

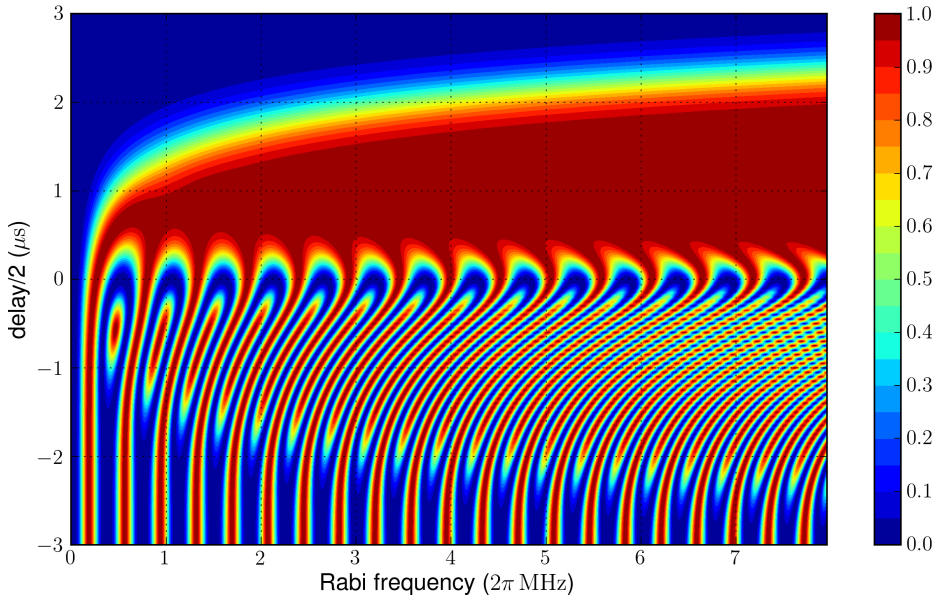

(a) Fidelity of the transfer to the target final state $|3\rangle$.

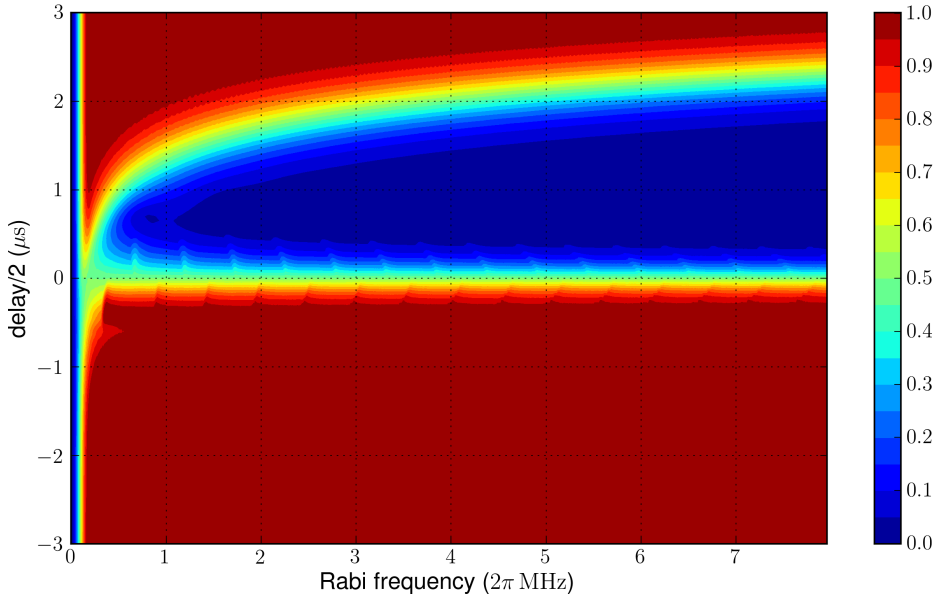

(b) Maximum population in the intermediate state $|2\rangle$ during the evolution.

Figure 5.1: Robustness of STIRAP with no losses. Gaussian pulses as defined in Eqs. (5.3) are used, and $\Gamma = 0$. Fig. (a) represents the fidelity F of the target final state; Fig. (b) represents the maximum of population m found in the intermediate state during the evolution. These functions are plotted against the equal maximum Rabi frequencies of the pump and Stokes pulses and the parameter τ which is half of the delay. Negative delays means that the pump pulse arrives before the Stokes pulse.

5.1.2 STIRAP with low losses

Consider the case

$$\Gamma = \frac{1}{T} = \frac{2}{3}\,\mu\mathrm{s}^{-1} = 2\pi \cdot 0.106\,\mathrm{MHz}. \tag{5.6}$$

This is the case in which the decay rate of the intermediate state $|2\rangle$ is of the order of T^{-1}.

The results of the numerical simulations are plotted in Fig. 5.2: (a) represents the fidelity F of the process and (b) the population loss in the intermediate state during the evolution. In the non-STIRAP region ($\tau \leq 0$) a small sign of Rabi oscillations is still present: the population oscillates between states $|1\rangle$ and $|3\rangle$ through the state $|2\rangle$, the population in this state is lost with a decay rate of Γ and then not all the population can be transferred to the final state $|3\rangle$.

In the STIRAP region instead, there is a wide range of values for which no population is lost in the intermediate state. This happens because the dark state is created and the population is directly channeled to the final state. See Figs. 5.2a and 5.2b.

Counter-intuitive pulse sequence is a required condition for efficient population transfer with this kind of loss.

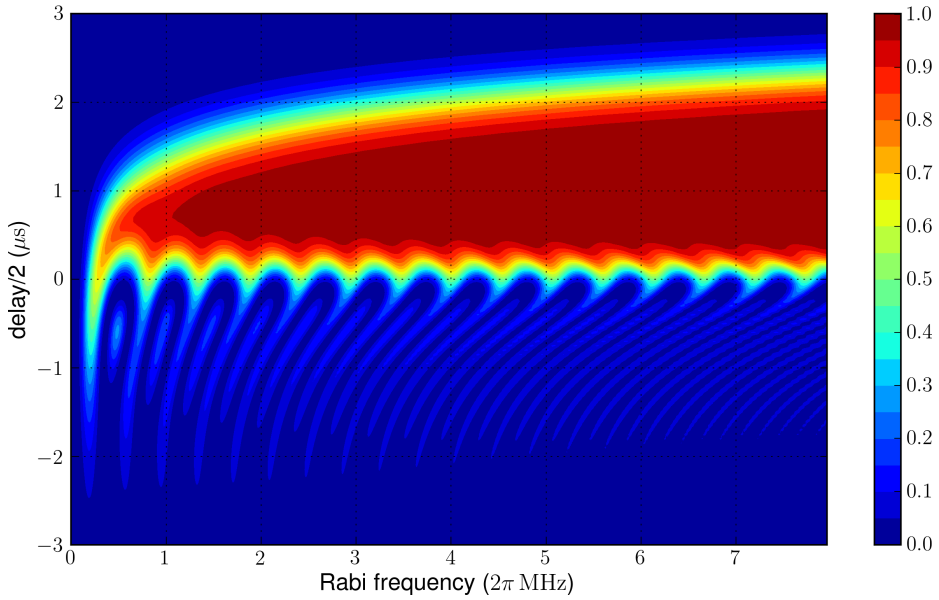

(a) Fidelity of the transfer to the target final state $|3\rangle$.

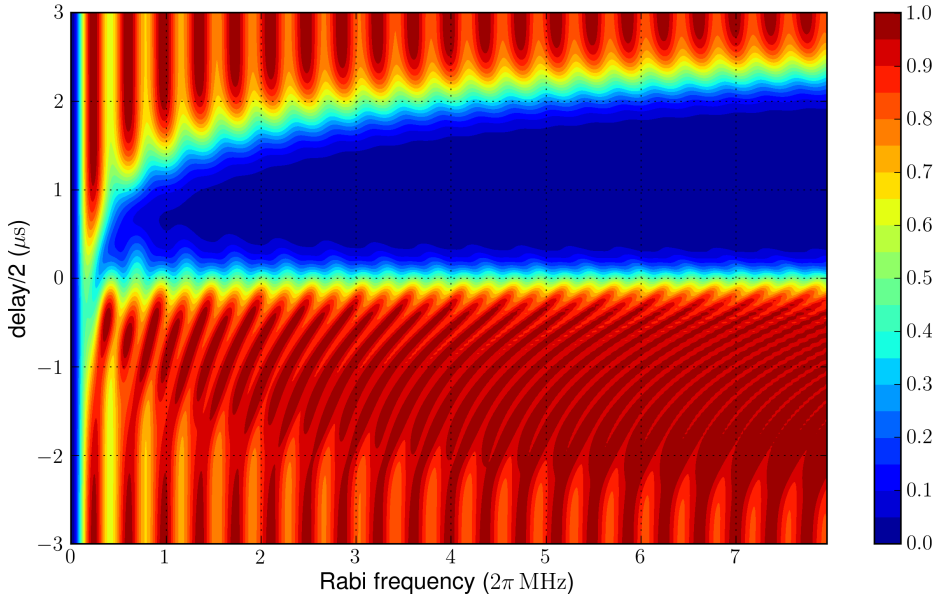

(b) Population loss in the intermediate state $|2\rangle$ during the evolution.

Figure 5.2: Robustness of STIRAP with low losses. Gaussian pulses are used and $\Gamma = 2\pi \cdot 0.106\,\mathrm{MHz}$. Fig. (a) represents the fidelity of the target final state; Fig. (b) represents the population decayed from the intermediate state $|2\rangle$. These functions are plotted against the equal maximum Rabi frequencies of the pump and Stokes pulses and the parameter τ which is half of the delay. Negative delays means that the pump pulse arrives before the Stokes pulse.

5.1.3 STIRAP with high losses

Consider the case

$$\Gamma = 10\frac{1}{T} = 10\frac{2}{3}\,\mu s^{-1} = 2\pi \cdot 1.061\,\mathrm{MHz} \tag{5.7}$$

This is the case in which the decay rate of the intermediate state $|2\rangle$ is greater then T^{-1}.

The results of the numerical simulations are plotted in Fig. 5.3: (a) represents the fidelity F of the process and (b) the population loss in the intermediate state during the evolution.

In this case there aren't Rabi oscillations because the population in the intermediate state decays with an high rate and does not reach the final state.

In Figs. 5.3a and 5.3b we see that for intuitive pulse sequence almost all the population is lost and that no population reach the final state.

However, with counter-intuitive pulse sequence, there are values for the Rabi frequency of the lasers and the delay, for which complete transfer can be reached and there is not loss in the intermediate state. This is due, again, to the creation of the dark state.

Counter-intuitive pulse sequence is a required condition for efficient population transfer also with this kind of loss.

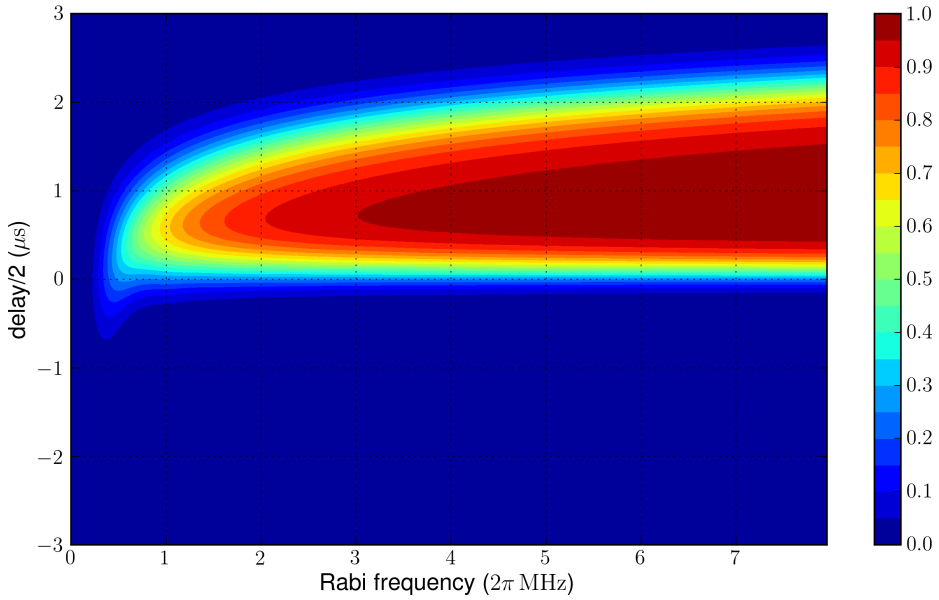

(a) Fidelity of the transfer to the target final state $|3\rangle$.

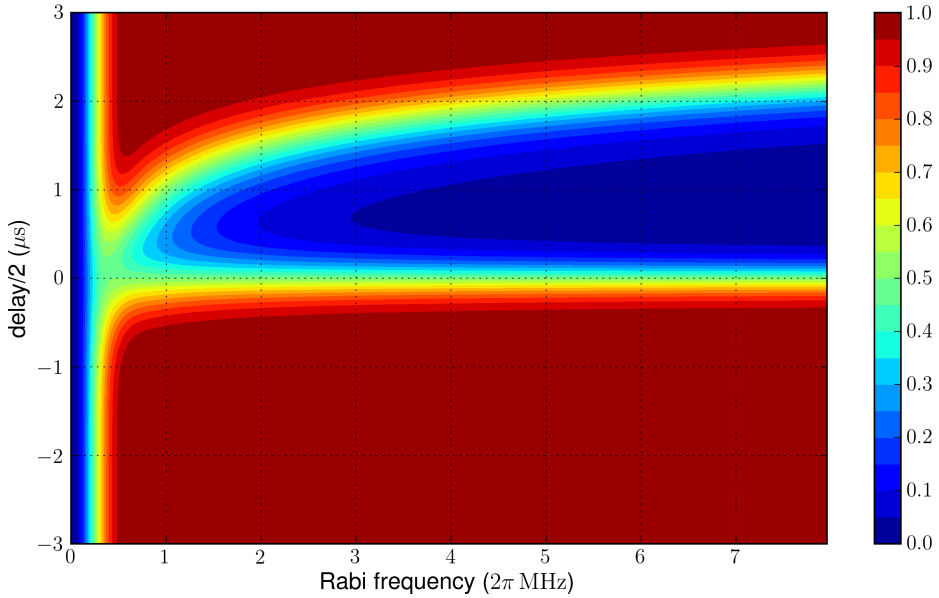

(b) Population loss in the intermediate state $|2\rangle$ during the evolution.

Figure 5.3: Robustness of STIRAP with high losses. Gaussian pulses are used and $\Gamma = 2\pi \cdot 1.061\,\mathrm{MHz}$. Fig. (a) represents the fidelity of the target final state; Fig. (b) represents the population decayed from the intermediate state $|2\rangle$. These functions are plotted against the equal maximum Rabi frequencies of the pump and Stokes pulses and the parameter τ which is half of the delay. Negative delays means that the pump pulse arrives before the Stokes pulse.

5.2 Super-Adiabatic STIRAP

Within the super-adiabatic expansion scheme for STIRAP, in addition to the pump and Stokes Rabi frequency $\Omega_p(t)$ and $\Omega_s(t)$, there is another interaction (see Sec. 3.2)

$$\Omega_d(t) = 2\frac{\dot{\Omega}_p(t)\Omega_s(t) - \Omega_p(t)\dot{\Omega}_s(t)}{\Omega_p(t)^2 + \Omega_s(t)^2} \tag{5.8}$$

the detuning pulse, which connect the initial with the final state.

With Gaussian pulses given in Eqs. (5.3) the detuning pulse is

$$\Omega_d(t) = \frac{4\tau}{T^2 \cosh\left(\frac{4t\tau}{T^2}\right)}. \tag{5.9}$$

We split the problem in the following manner:

1. we fix $\Omega_d(t)$, and we vary the parameters of $\Omega_p(t)$ and $\Omega_s(t)$,
2. we fix $\Omega_p(t)$ e $\Omega_s(t)$, and we let vary $\Omega_d(t)$ from the optimal values.

Consider only the case $\tau > 0$, which is exactly the super-adiabatic STIRAP. In the preceding section we considered also the case with $\tau \leq 0$, but within the super-adiabatic scheme it makes no sense because with that condition the dark state does not connect the state $|1\rangle$ at t_i with the state $|3\rangle$ at t_f.

5.2.1 Robustness with respect to the pump and Stokes lasers

We fix $\Omega_d(t)$ (see Eq. (5.9)) with $T = 1.5\,\mu$s and $\tau = 0.7\,\mu$s. With $\Omega_p(t)$ and $\Omega_s(t)$ defined as in Eq. (5.3), we fix $T = 1.5\,\mu$s and we vary A and τ. As in the preceding section we study the cases without relaxation of the intermediate state ($\Gamma = 0$), with low relaxation ($\Gamma = T^{-1}$) and with high relaxation ($\Gamma = 10T^{-1}$).

Without relaxation

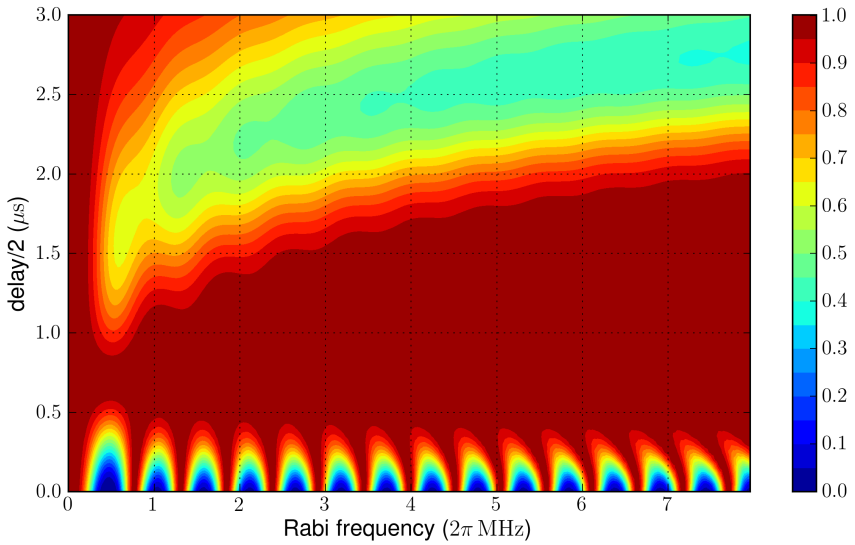

(a) Fidelity of the transfer to the target final state $|3\rangle$.

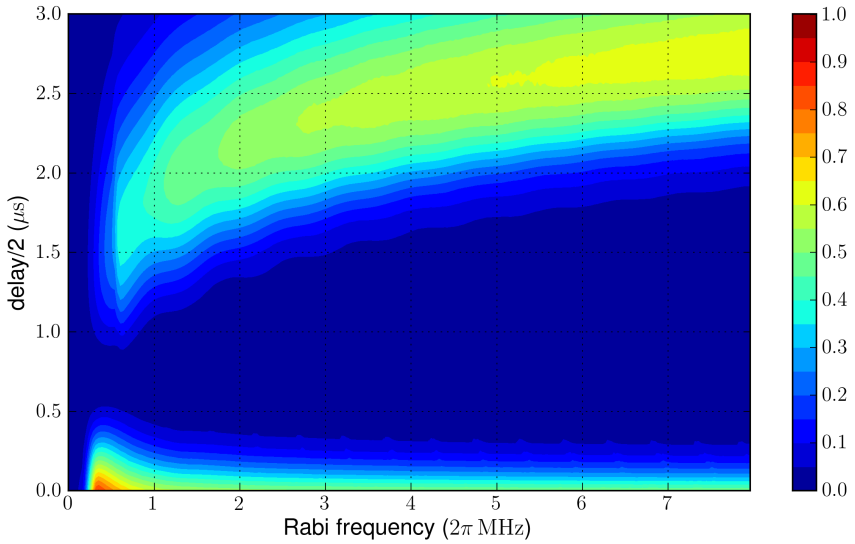

(b) Maximum population in the intermediate state $|2\rangle$ during the evolution.

Figure 5.4: Robustness of Super-Adiabatic STIRAP with no losses, $\Gamma = 0$. The functions F and m are plotted against the maximum Rabi frequencies of the pump and Stokes pulses and the parameter τ which is half of the delay.

With low losses

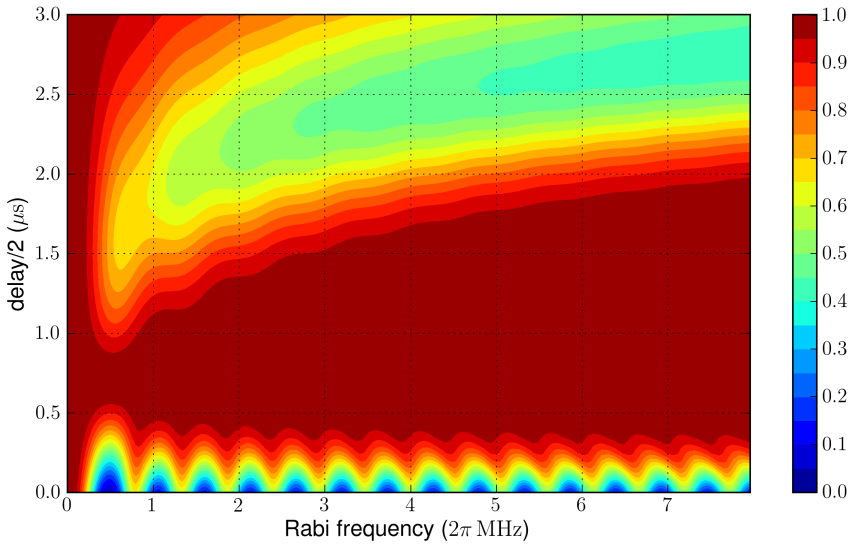

(a) Fidelity for the target final state $|3\rangle$.

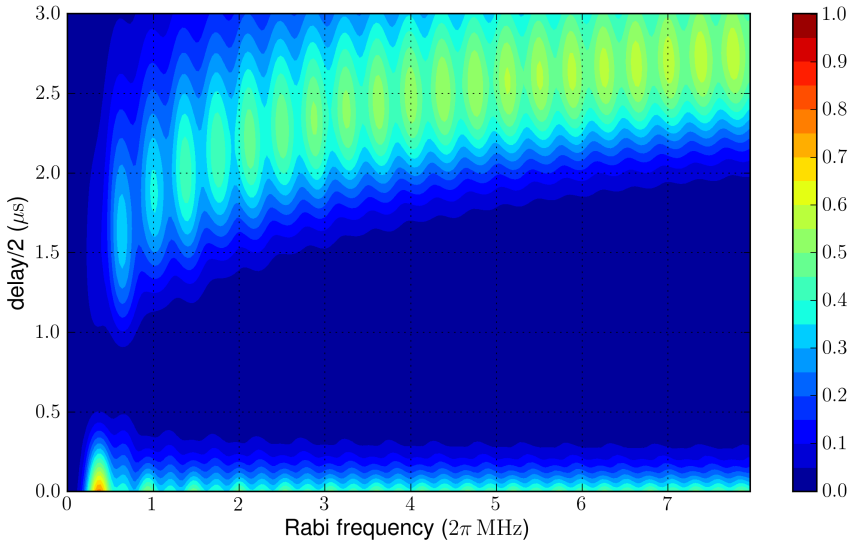

(b) Population loss in the intermediate state $|2\rangle$ during the evolution.

Figure 5.5: Robustness of Super-Adiabatic STIRAP with low loss, $\Gamma = T^{-1}$. The functions are plotted against the equal maximum Rabi frequencies of the pump and Stokes pulses and the parameter τ which is half of the delay.

With high losses

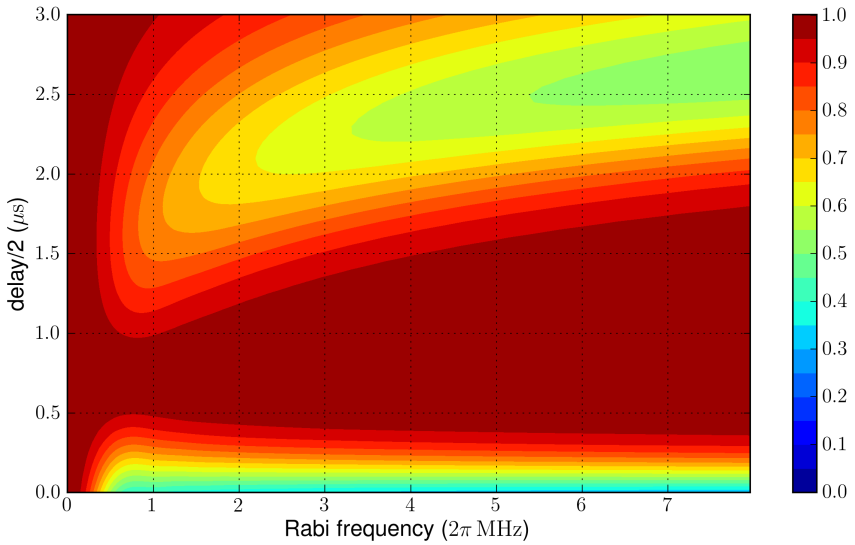

(a) Fidelity of the transfer to the target final state $|3\rangle$.

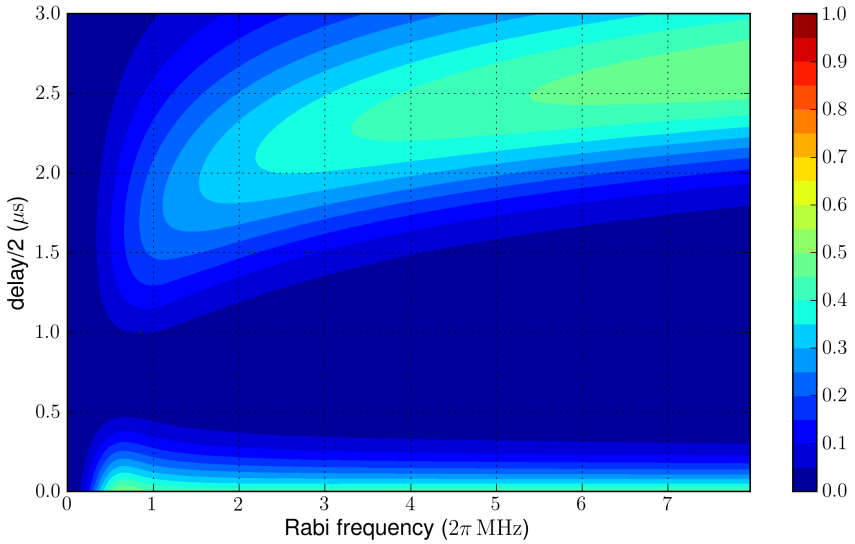

(b) Population loss in the intermediate state $|2\rangle$ during the evolution.

Figure 5.6: Robustness of Super-Adiabatic STIRAP with high loss, $\Gamma = 10T^{-1}$. The functions are plotted against the equal maximum Rabi frequencies of the pump and Stokes pulses and the parameter τ which is half of the delay.

5.2.2 Comparison between STIRAP and Super-Adiabatic STIRAP

In Fig. 5.7 are reported the expansion of Figs. 5.2a and 5.5a around the fidelity $F = 1$. In this region the detuning pulse improve the STIRAP robustness and increase the fidelity of the transfer to the final state.

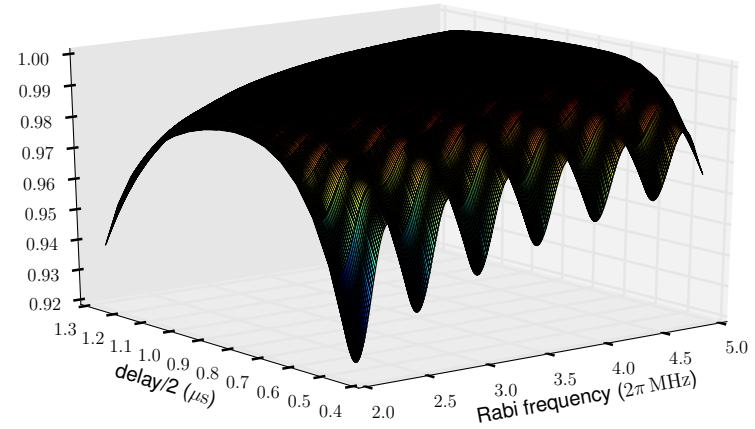

(a) Fidelity of the STIRAP process with low loss, expansion around $F = 1$.

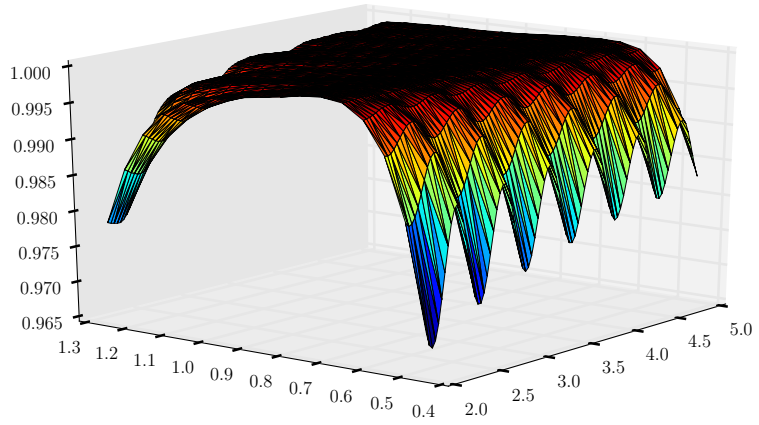

(b) Fidelity of the Super-Adiabatic STIRAP process with low loss, expansion around $F = 1$.

Figure 5.7: Comparison between the fidelity of the STIRAP and the Super-Adiabatic STIRAP process around the maximum value of fidelity $F = 1$.

5.2.3 Robustness with respect to the detuning pulse

In this case we fix $T = 1.5\,\mu$s and $\tau = 0.7\,\mu$s. For various values of the pump and Stokes maximum Rabi frequency, we study the robustness varying the delay and the area of the detuning pulse from their optimal values. Their optimal values are obtained from the definition (5.9) and are zero delay and area equal to π.

We study only the more difficult case of high relaxation from the intermediate state.

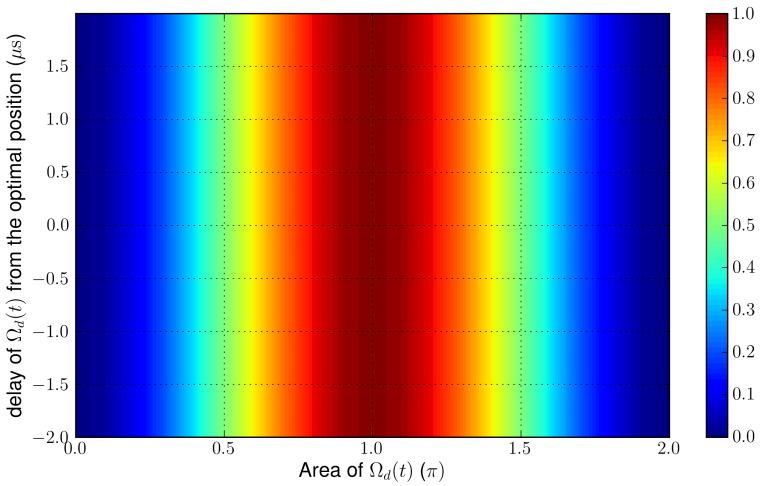

Figure 5.8: Fidelity of the transfer with $A = 0$.

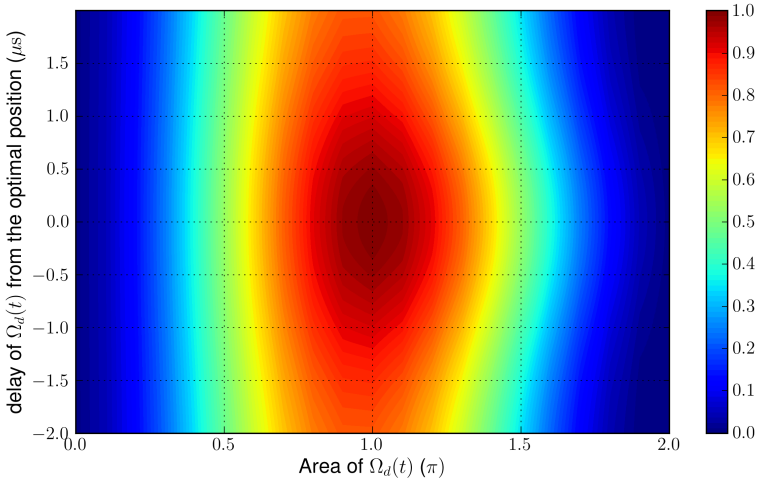

Figure 5.9: Fidelity of the transfer with $A = 0.16 \cdot 2\pi$MHz.

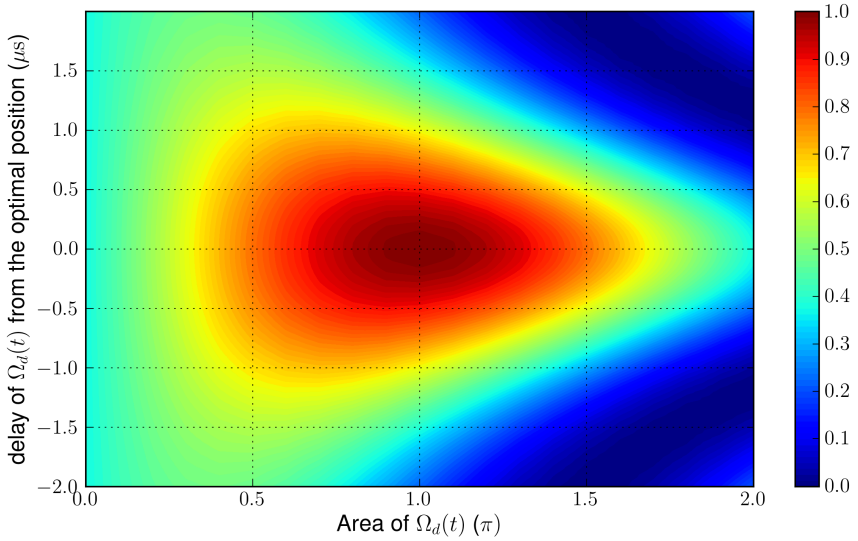

Figure 5.10: Fidelity of the transfer with $A = 0.64 \cdot 2\pi$MHz.

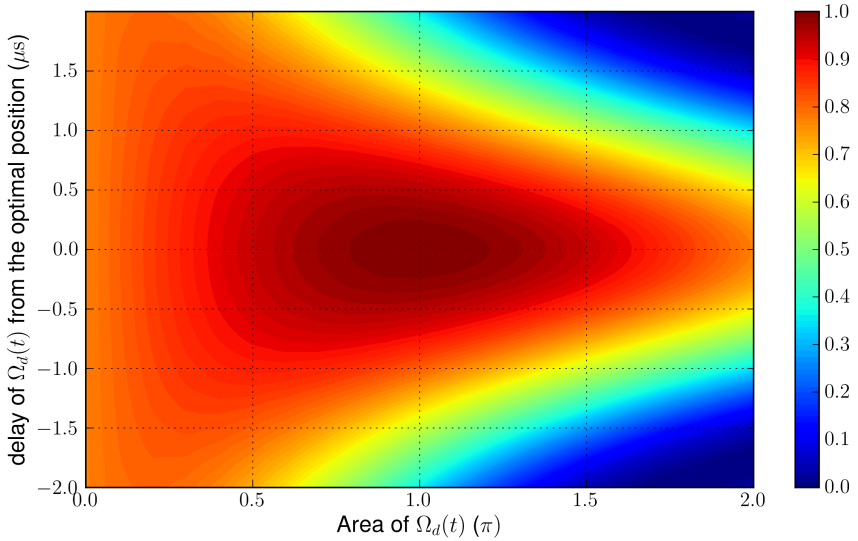

Figure 5.11: Fidelity of the transfer with $A = 1.27 \cdot 2\pi$MHz.

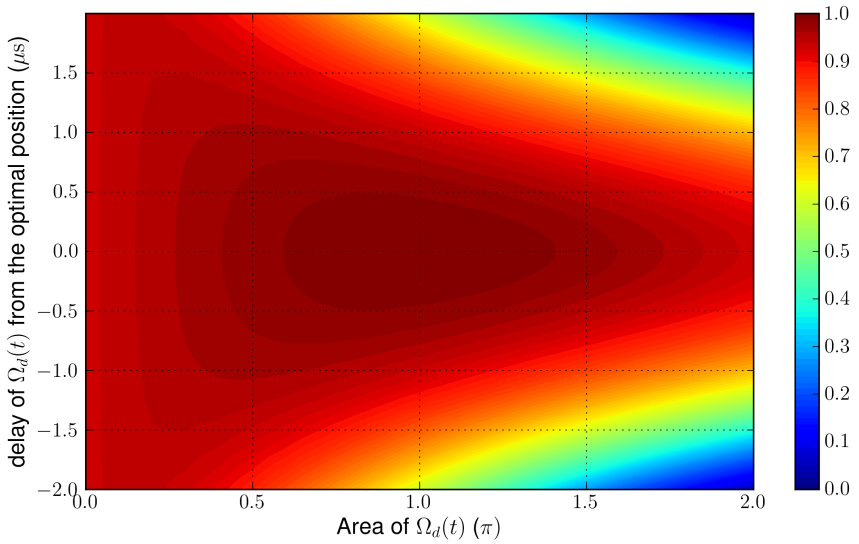

Figure 5.12: Fidelity of the transfer with $A = 2.55 \cdot 2\pi$MHz.

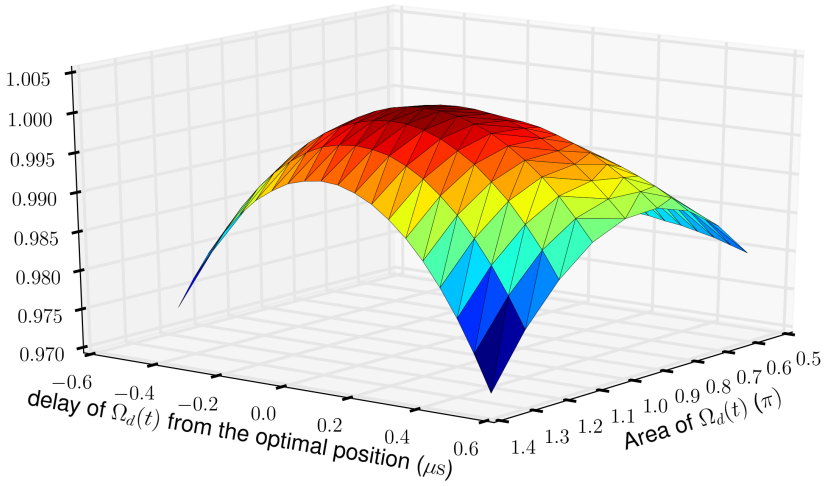

Figure 5.13: Fidelity of the transfer with $A = 2.55 \cdot 2\pi$MHz, expansion around $F = 1$.

Now we fix the delay of the detuning pulse to its optimal value (with definition given in this chapter its optimal value is 0) and we study the robustness with respect to the area of the detuning pulse and to the equal maximum Rabi frequencies of the pump and Stokes laser.

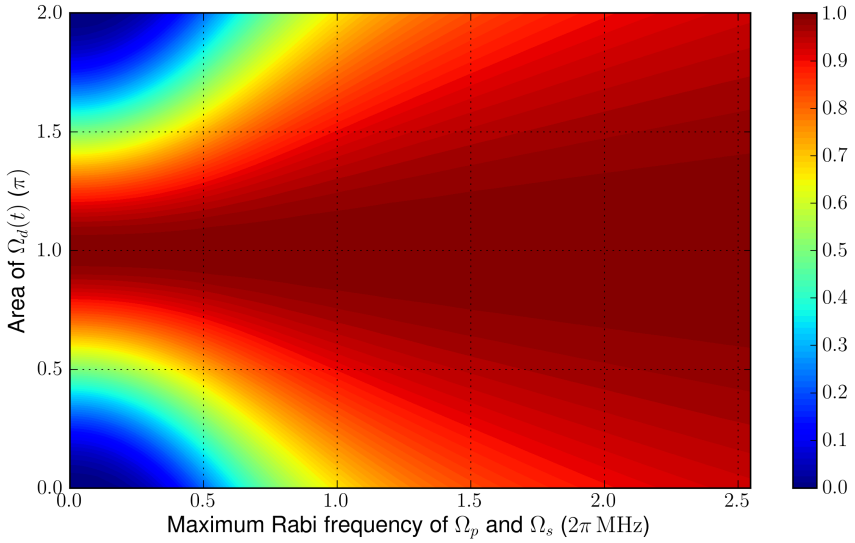

Figure 5.14: Fidelity of the transfer as a function of the detuning pulse area and of the equal maximum Rabi frequencies of the pump and Stokes pulses. The optimal value for the detuning pulse area is π.

Fig. 5.14 shows that the pump and Stokes pulses makes the detuning pulse, which is a π-pulse, more robust to variation of its area. The same thing can be seen by comparing Figs. 5.8, 5.9, 5.10, 5.11 and 5.12.

It is interesting to test the robustness also of the phase of the detuning pulse. As seen in section 3.2.2 the phase of the detuning pulse has to have an established value for the transfer to be super-adiabatic. Fig. 5.15 represent the fidelity of the transfer with respect to the variation of the equal maximum Rabi frequencies of the pump and Stokes pulses and to the variation of the phase of the detuning pulse from its optimal value.

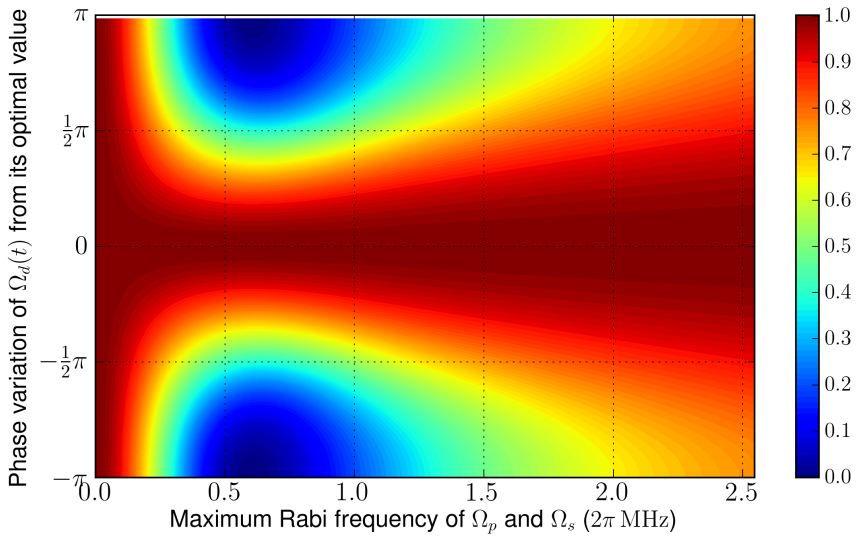

Figure 5.15: Fidelity of the transfer as a function of the equal maximum Rabi frequencies of the pump and Stokes pulses and of the variation of the phase of the detuning pulse from its optimal value.

Fig. 5.15 shows that variations of the order of $\pi/10$ of the phase of the detuning pulse from its optimal value can prevent the complete transfer of population to the final state. However, the range of values around the optimal one that the phase can assume without preventing the complete transfer becomes larger for larger values of Rabi frequencies of the pump and Stokes pulses.

CHAPTER 6

Experimental Study

In the BEC lab the STIRAP was applied to excite ^{87}Rb atoms to Rydberg states using a ladder level scheme. The target of the experimental work was to perform for the first time an absolute test of the STIRAP efficiency, accessible to the lab owing to the accurate determination of the number of atoms and the number of Rydberg [16]. A preliminary investigation was performed for a period of two-months and I participated to the experimental plan and to the data collection.

The initial state $|1\rangle$ is the ground state $5^2S_{1/2}$, the intermediate state $|2\rangle$ is the state $6^2P_{3/2}$ and the final target state $|3\rangle$ is the Rydberg state $70^2S_{1/2}$. The hyperfine structure for the two lower states has to be taken into account. Furthermore, a magnetic field removes the degeneracy from each hyperfine level (Zeeman effect). The two lower states used are $|F = 2,\, m_F = 2\rangle$ for the ground state and $|F = 3,\, m_F = 3\rangle$ for the intermediate state. For the Rydberg state is used the level $|J = 1/2, m_J = 1/2\rangle$.

6.1 Rydberg Atoms

Rydberg atoms are atoms excited to high energy states, characterized by large principal quantum number n.

A Rydberg atom can be described as an electron orbiting around the atomic core. This electron "feels" mainly the Coulomb potential of the Z protons in the nucleus shielded by $Z - 1$ core electrons. This configuration resembles hydrogen and therefore, a lot of the properties of Rydberg atoms can be derived from the hydrogen atom approach. The energy and radius of hydrogen atom with an electron in a state with principal quantum number n are given by

$$E_n = -R_\infty \frac{hc}{n^2}, \tag{6.1a}$$

$$r_n = a_0 n^2, \tag{6.1b}$$

where a_0 is the Bohr radius and R_∞ is the Rydberg constant

$$R_y = hcR_\infty = \frac{\hbar^2}{2m_e a_0^2} \approx 13.6\,\text{eV} \tag{6.2}$$

Rydberg states with small angular momentum $l < 4$ are called *defect states*. The defect is due to the energy shift caused by the core electrons. This shift has to be taken into account by replacing the principal quantum number n with an effective principal quantum number $n^* = n - \delta_l$. The quantum defect δ_l , can be calculated with the Rydberg-Ritz formula [32]. The quantum defect for Rydberg states of Rb with zero angular momentum (S-states) is $\delta_0 \approx 3.13$.

The radius of an excited atom scales like n^2 and can hence become very large (for $n = 100$ about one μm) compared to the atom in a ground state (order of nm). The large distance of the electron from the atomic core determines most of the physical properties of Rydberg atoms.

Atoms that are excited to Rydberg states are subject to spontaneous emission. The total radiative decay rate of a Rydberg state at temperature T, is constituted by two radiative depopulation effects

$$\frac{1}{\tau_{eff}(T)} = \frac{1}{\tau_0} + \frac{1}{\tau_{BBR}(T)}. \tag{6.3}$$

The term $1/\tau_0$ is due to radiative decay to lower lying states at $T = 0$, the term $1/\tau_{BBR}$ is due to depopulation induced by thermal radiation.

The lifetime τ_0 increases as n or l increases and can be accurately calculated using the empiric formula [32]

$$\tau_0 = \tau'(n^*)^\gamma. \tag{6.4}$$

Table 6.1 reports some values of the parameters τ' and γ for Rb atoms.

The blackbody depopulation lifetime is [32]

$$\frac{1}{\tau_{BBR}(T)} = \frac{4\alpha^3 k_B T}{3(n^*)^2} \tag{6.5}$$

with α the fine structure constant and k_B the Boltzmann constant. Accurate value of the blackbody lifetime are reported in Ref. [33].

For instance for the $70^2S_{1/2}$ state of the STIRAP investigation, Beterov et al. [33] report a value of 151.55 μs for τ_{eff} at 300 K.

Parameter	s	p	d	f
τ'(ns)	1.43	2.76	2.09	0.76
γ	2.94	3.02	2.85	2.95

Table 6.1: Lifetime parameters of Eq. (6.4) for Rb atoms [32].

6.2 Experimental Set-up and Protocol

^{87}Rb atoms are cooled in magneto-optical trap (MOT) to temperatures of the order of $100\,\mu$K. Fig. 6.1 reports the energy levels for the Rb laser cooling scheme, with the ground and excited hyperfine states denoted as $|F\rangle$ and $|F'\rangle$. The optical transition used to cool atoms is the $5^2S_{1/2} - 5^2P_{3/2}$ transition (D2 line). The hyperfine levels used for this transition are the $|F = 2\rangle$ for the ground state and $|F' = 3\rangle$ for the excited state. It means that only the atoms in the $|F = 2\rangle$ level are trapped in the MOT. However, atoms can be off-resonantly excited to the $|F' = 2\rangle$ level, where they may decay to $|F = 1\rangle$. This decay may cause losses of atoms from the MOT. To avoid this, a laser with light near-resonant to the $|F = 1\rangle \rightarrow |F' = 2\rangle$ transition is added to the laser cooling light. This laser re-pump atoms from the $|F = 1\rangle$ level to the $|F = 2\rangle$ one.

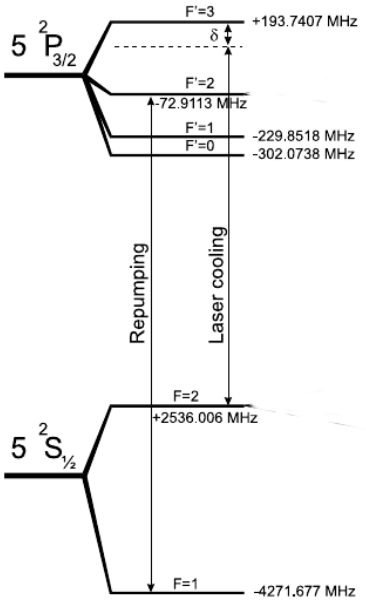

Figure 6.1: Scheme of laser cooling in the D2 line of ^{87}Rb.

As in Fig. 6.2 the STIRAP process requires two laser fields. The pump laser of wavelength 421 nm and polarization σ^+ is obtained by doubling the frequency of a 842 nm TA100 laser by TOPTICA. As mentioned before, it couples the states $\left|5^2S_{1/2},\, F = 2,\, m_F = 2\right\rangle$ and $\left|6^2P_{3/2},\, F = 3,\, m_F = 3\right\rangle$. The Stokes pulse is accomplished by IR laser light at wavelength of 1012 nm and polarization σ^-. It should couple the states $\left|6^2P_{3/2},\, F = 3,\, m_F = 3\right\rangle$ and $\left|70^2S_{1/2},\, m_J = 1/2\right\rangle$. In order to perform the STIRAP investigation, circular polarisers were inserted into the optical path of both lasers. However, the achieved degree of polarization was not good enough for an efficient STIRAP, as the results presented in the following will demonstrate.

In a MOT the cooled atoms occupy all the Zeeman sublevels, while the STIRAP

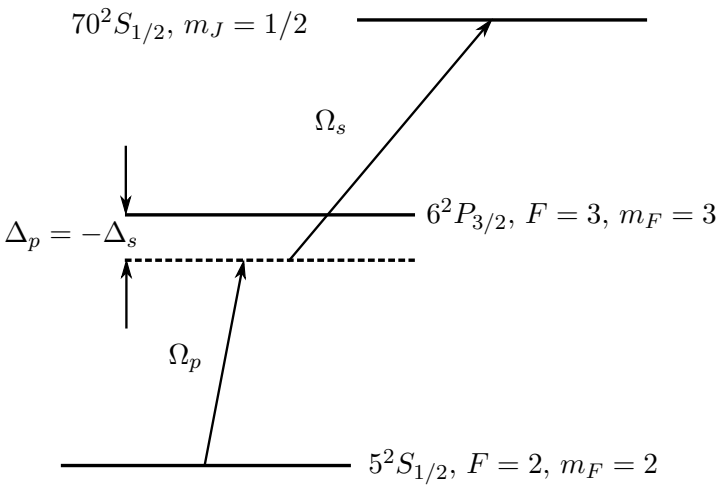

Figure 6.2: Energy level scheme for the STIRAP experimental investigation in ^{87}Rb

requires the preparation of the single $\left|5^2S_{1/2},\, F = 2,\, m_F = 2\right\rangle$ state. To accomplish this preparation through optical pumping, a magnetic field is required. For convenience a magnetic field already present in the experimental apparatus is used. It is called "TOP" (*Time Orbiting Potential*) and it rotates at a frequency

$$\frac{\omega}{2\pi} = 10\,\mathrm{KHz}. \tag{6.6}$$

The maximum value of this field is $B = 38\,\mathrm{G}$. During the experimental sequence this magnetic field takes three values 0, $B0 \approx 1\,\mathrm{G}$ and $B1 \approx 10 - 20\,\mathrm{G}$. The value $B0$ is needed to lower the density of the atoms in the MOT. The value $B2$ generates Zeeman splitting between hyperfine levels during the laser pulses needed for STIRAP. During the detection of the Rydberg states the magnetic field is turned off to maximize the efficiency of the detection.

The series of signals that control laser pulses and magnetic fields are schematized in Fig. 6.3. First $10^2 - 10^3$ atoms are trapped in the MOT, then the MOT lasers and magnetic fields are switched off. The TOP magnetic field is raised to the value $B1$ and three optical pumping pulses act on the system to pump atoms in the ground state $\left|5^2S_{1/2},\, F = 2,\, m_F = 2\right\rangle$ level. During the optical pumping the re-pump laser is held on. After the three pulses of optical pumping the STIRAP pulses are applied. We use two Gaussian Pulses as in Eq. (6.7) with $T = 0.5\,\mu$s, and we vary the delay between them from $-2\,\mu$s (intuitive pulse sequence) to $2\,\mu$s (counter-intuitive pulse sequence). After the STIRAP pulses, the TOP field is turned off, it takes about $30\,\mu$s to became negligible. Then the detection process starts: the Rydberg states are ionized via an electric field and are collected in the channeltron.

The optical pumping light has horizontal direction, while the pump and the Stokes pulses are collinear and form an angle of 11° with the direction of the optical pumping

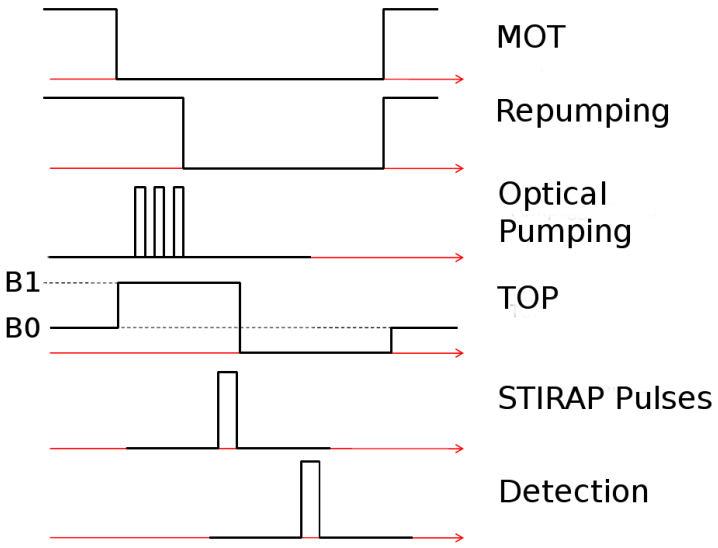

Figure 6.3: Experimental sequence.

light. All this pulses are synchronized with the TOP magnetic field such that this rotating field is in parallel to the optical-pumping/STIRAP quantisation axis when the pulses are applied.

6.3 Experimental Results

All states of the ^{87}Rb atom interesting for the process are represented in Fig. 6.4. There are the three states of interest $5^2S_{1/2}$, $6^2P_{3/2}$ and $70^2S_{1/2}$, and other three states useful to describe the relaxation process: $6^2P_{1/2}$, $4D$ and $5S$.

In Fig. 6.5 the data acquired in an experimental test are reported. Gaussian pulses have been used

$$\begin{aligned} \Omega_p(t) &= Ae^{-\left(\frac{t-\tau}{T}\right)^2} \\ \Omega_s(t) &= Be^{-\left(\frac{t+\tau}{T}\right)^2} \end{aligned} \tag{6.7}$$

with $T = 0.5\,\mu$s, $A = 2\pi \cdot 2.8\,$MHz and $B = 2\pi \cdot 0.9\,$MHz. The number of atoms collected in the MOT for this experiment is 1500. Each point in the graph is the mean of four cycle of measures. Each cycle consist in 20 measures of the number of Rydberg states created at the end of the STIRAP pulses. The time elapsed between two acquisitions is one second.

The comparison of experimental data with theoretical expectation are represented in Fig. 6.6. In this graph the efficiency of detection of ions in the channeltron (about 40%) is taken into account. Theoretical predictions for the open system of Fig. 6.4 are reported. In this simulation the coherence of lasers' light has been taken into account by

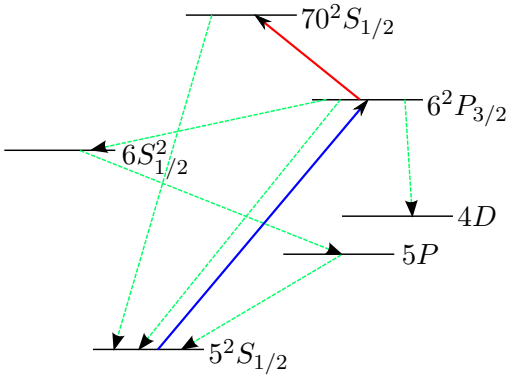

Figure 6.4: Rubidium level scheme. The blue arrow is the pump field, the red arrow is the Stokes field. The green dashed lines represent the spontaneous decay between atomic states. This system is open because the population that decays in the level $5^2S_{1/2}$, $F = 1$ is loss.

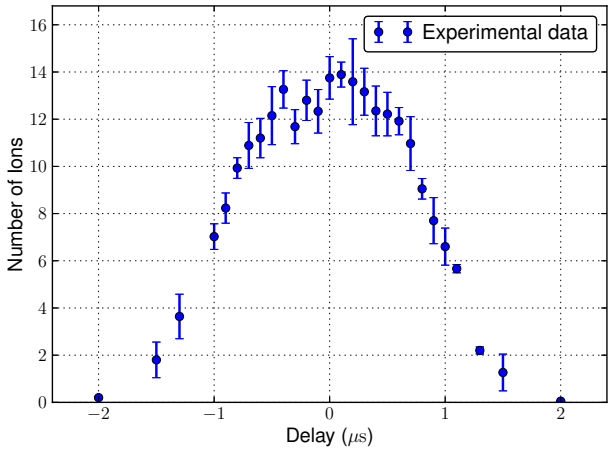

Figure 6.5: STIRAP experimental results vs the laser pulse delay for the parameters reported in the text.

introducing this decoherence factors: $\Gamma_p = \Gamma_s = 0.3 \cdot (2\pi\,\mathrm{MHz})$ and $\Gamma_{cross} = 1 \cdot (2\pi\,\mathrm{MHz})$.
Two main differences appear from the comparison:

1. The theory predicts a transfer efficiency larger by a factor 4 than the measured one.

2. The STIRAP maximum at a positive delay does not appear in the experimental result.

Several tests performed in the laboratory have verified that while parameters as the magnetic field, the optical pumping and the collection efficiency were correctly chosen, the polarization of the IR laser was not perfect as required for a three-level scheme.

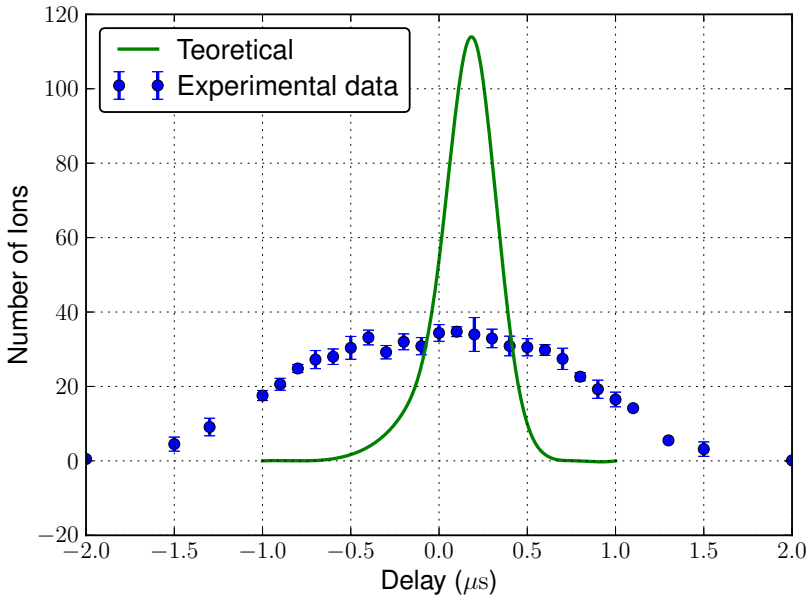

Figure 6.6: STIRAP preliminary results. Comparisons with theoretical results.

Therefore the experiment will be repeated when good polarisers for the IR lasers will be purchased. From the theoretical side a simulation including the full Zeeman degeneracy may be performed in the near future in order to verify if the non correct polarisation is the critical issue.

Conclusions

STIRAP is a very robust method to achieve complete population transfer. However its implementation is not simple due to the requirement of high light intensity and high coherence time of used lasers.

Its super-adiabatic expansion, the Super-Adiabatic STIRAP, adds a new interaction between the initial and final state (the detuning pulse). This new interaction is a π-pulse and there must be a defined phase relation between it and the pump and Stokes lasers. This requirements are very difficult to achieve. However, also if these requirements are not completely satisfied, the presence of detuning pulse improves the fidelity and the robustness of the simple STIRAP. From an other point on view, we can also say that the STIRAP pulses enhance the robustness of the π-pulse, which alone, as seen, is very sensitive to variation of parameters.

Experimental research about the super-adiabatic STIRAP is an interesting task, but it will require almost absolute control of the laser light used in the system.

Bibliography

[1] I. Walmsley and H. Rabitz. "Quantum Physics Under Control". In: *Physics Today* 56.8 (2003), pp. 43–49.

[2] Michael A. Nielsen and Isaac L. Chuang. *Quantum Computation and Quantum Information*. Cambridge University Press, 2000. ISBN: 9780521635035.

[3] C.E. Hamilton, J.L. Kinsey, and R.W. Field. "Stimulated emission pumping - New methods in spectroscopy and molecular dynamics". English. In: *Annual Review of Physical Chemistry* 37 (1986), 493–524. ISSN: 0066-426X.

[4] K. Bergmann and B.W. Shore. "Coherent Population Transfer". In: *Molecular Dynamics and Spectroscopy by Stimulated Emission Pumping*. 1995. Chap. 9, pp. 315–373.

[5] K. Bergmann, H. Theuer, and B.W. Shore. "Coherent population transfer among quantum states of atoms and molecules". In: *Rev. Mod. Phys.* 70 (3 July 1998), pp. 1003–1025.

[6] T. Cubel, B. K. Teo, V. S. Malinovsky, J. R. Guest, A. Reinhard, B. Knuffman, P. R. Berman, and G. Raithel. "Coherent population transfer of ground-state atoms into Rydberg states". In: *Phys. Rev. A* 72.2 (Aug. 2005), pp. 023405–+.

[7] M. A. Gearba, H. A. Camp, M. L. Trachy, G. Veshapidze, M. H. Shah, H. U. Jang, and B. D. DePaola. "Measurement of population dynamics in stimulated Raman adiabatic passage". In: *Phys. Rev. A* 76 (1 July 2007), p. 013406.

[8] R. Lim and M. V. Berry. "Superadiabatic tracking of quantum evolution". In: *Journal of Physics A: Mathematical and General* 24.14 (1991), p. 3255.

[9] M.V. Berry. "Transitionless quantum driving". In: *Journal of Physics A: Mathematical and Theoretical* 42.36 (2009), p. 365303.

[10] M. Demirplak and S. A. Rice. "Adiabatic Population Transfer with Control Fields". In: *The Journal of Physical Chemistry A* 107.46 (2003), pp. 9937–9945.

[11] M. Demirplak and S. A. Rice. "On the consistency, extremal, and global properties of counterdiabatic fields". In: *The Journal of Chemical Physics* 129.15, 154111 (2008), p. 154111.

[12] E. Torrontegui, S. Ibáñez, S. Martínez-Garaot, M. Modugno, A. del Campo, D. Guéry-Odelin, A. Ruschhaupt, Xi Chen, and J. G. Muga. "Chapter 2 - Shortcuts to Adiabaticity". In: *Advances in Atomic, Molecular, and Optical Physics*. Ed. by Paul R. Berman Ennio Arimondo and Chun C. Lin. Vol. 62. Advances In Atomic, Molecular, and Optical Physics. Academic Press, 2013, pp. 117–169.

[13] M. G. Bason, M. Viteau, N. Malossi, P. Huillery, E. Arimondo, D. Ciampini, R. Fazio, V. Giovannetti, R. Mannella, and O. Morsch. "High-fidelity quantum driving". In: *Nature Phys. 8, 147-152 (2012)* (Nov. 2011).

[14] N. Malossi, M. G. Bason, M. Viteau, E. Arimondo, R. Mannella, O. Morsch, and D. Ciampini. "Quantum driving protocols for a two-level system: From generalized Landau-Zener sweeps to transitionless control". In: *Phys. Rev. A* 87 (1 Jan. 2013), p. 012116.

[15] N. Malossi, M. G. Bason, M. Viteau, E. Arimondo, D. Ciampini, R. Mannella, and O. Morsch. "Quantum driving of a two level system: quantum speed limit and superadiabatic protocols – an experimental investigation". In: *Journal of Physics: Conference Series* 442.1 (2013), p. 012062.

[16] M. Viteau, M. G. Bason, J. Radogostowicz, N. Malossi, D. Ciampini, O. Morsch, and E. Arimondo. "Rydberg Excitations in Bose-Einstein Condensates in Quasi-One-Dimensional Potentials and Optical Lattices". In: *Phys. Rev. Lett.* 107 (6 Aug. 2011), p. 060402.

[17] M. Born and V. Fock. "Beweis des Adiabatensatzes". German. In: *Zeitschrift für Physik* 51.3-4 (1928), pp. 165–180. ISSN: 0044-3328.

[18] A. Messiah. *Quantum mechanics, Vol. 1/2*. North-Holland, Amsterdam, 1961.

[19] E. Arimondo and G. Orriols. "Nonabsorbing atomic coherences by coherent two-photon transitions in a three-level optical pumping". In: *Lettere Al Nuovo Cimento Series 2* 17.10 (1976), p. 333. ISSN: 1827-613X.

[20] E. Arimondo. "Coherent Population Trapping in Laser Spectroscopy". In: ed. by E. Wolf. Vol. 35. Progress in Optics. Elsevier, 1996, pp. 257–354.

[21] B.W. Shore. *The theory of coherent atomic excitation*. 1990.

[22] V.I Romanenko and L.P Yatsenko. "Adiabatic population transfer in the three-level Λ-system: two-photon lineshape". In: *Optics Communications* 140.4–6 (1997), pp. 231–236. ISSN: 0030-4018.

[23] M.P. Fewell, B.W. Shore, and K. Bergmann. "Coherent population transfer among three states: Full algebraic solutions and the relevance of non adiabatic processes to transfer by delayed pulses". In: *Australian journal of physics* 50.2 (1997), pp. 281–308.

[24] J.R. Kuklinski, U. Gaubatz, F.T. Hioe, and K. Bergmann. "Adiabatic population transfer in a three-level system driven by delayed laser pulses". In: *Physical Review A* 40 (1989), pp. 6741–6744.

[25] X. Chen, I. Lizuain, A. Ruschhaupt, D. Guéry-Odelin, and J.G. Muga. "Shortcut to adiabatic passage in two-and three-level atoms". In: *Physical review letters* 105.12 (2010), p. 123003.

[26] R.G Unanyan, L.P Yatsenko, K. Bergmann, and B.W Shore. "Laser-induced adiabatic atomic reorientation with control of diabatic losses". In: *Optics Communications* 139.1–3 (1997), pp. 48–54. ISSN: 0030-4018.

[27] M. Fleischhauer, R. Unanyan, B.W. Shore, and K. Bergmann. "Coherent population transfer beyond the adiabatic limit: Generalized matched pulses and higher-order trapping states". In: *Phys. Rev. A* 59 (5 May 1999), pp. 3751–3760.

[28] H. Metcalf and P. van der Straten. *Laser Cooling and Trapping*. Springer, 1999.

[29] E. Brion, L. H. Pedersen, and K. Mølmer. "Adiabatic elimination in a lambda system". In: *Journal of Physics A: Mathematical and Theoretical* 40.5 (2007), p. 1033.

[30] T.A. Laine and S. Stenholm. "Adiabatic processes in three-level systems". In: *Physical Review A* 53.4 (1996), p. 2501.

[31] C.E. Carroll and F.T. Hioe. "Analytic solutions for three-state systems with overlapping pulses". In: *Physical Review A* 42.3 (1990), p. 1522.

[32] T. F. Gallagher. *Rydberg Atoms*. Cambridge: Cambridge University Press, 1994.

[33] I. I. Beterov, I. I. Ryabtsev, D. B. Tretyakov, and V. M. Entin. "Quasiclassical calculations of blackbody-radiation-induced depopulation rates and effective lifetimes of Rydberg nS , nP , and nD alkali-metal atoms with n<80". In: *Phys. Rev. A* 79.5 (May 2009), p. 052504.